NASA CONTRACTOR
REPORT

NASA CR-1

C. 1

PREDICTIONS ON THE CHARACTERISTICS OF THE MINIMAL TWO-IMPULSE ORBITAL TRANSFER UNDER ARBITRARY TERMINAL CONDITIONS BY USING THE BOUNDING TRAJECTORIES

by Fang Toh Sun

Prepared by
WICHITA STATE UNIVERSITY
Wichita, Kans. 67208
for

NATIONAL AERONAUTICS AND SPACE ADMINISTRATION • WASHINGTON, D. C. • OCTOBER 1971

1. Report No. NASA CR-1822	2. Government Accession No.	3. Recipient's Catalog No.
4. Title and Subtitle PREDICTIONS ON THE CHARACTERISTICS OF THE MINIMAL TWO-IMPULSE ORBITAL TRANSFER UNDER ARBITRARY TERMINAL CONDITIONS BY USING THE BOUNDING TRAJECTORIES		5. Report Date October 1971
		6. Performing Organization Code
7. Author(s) Fang Toh Sun		8. Performing Organization Report No.
		10. Work Unit No.
9. Performing Organization Name and Address Wichita State University Wichita, Kansas 67208		11. Contract or Grant No. NGR-17-003-008
		13. Type of Report and Period Covered Contractor Report
12. Sponsoring Agency Name and Address National Aeronautics and Space Administration Washington, D. C. 20546		14. Sponsoring Agency Code
15. Supplementary Notes		

16. Abstract

The characteristics of the minimal total impulse solution of the two-terminal, two-impulse orbital transfer problems are predicted. The terminal conditions are assumed arbitrary. The concept of bounding trajectories is applied, from which qualitative and quantitative information on the minimal total impulse transfer are deduced without solving the octic equation, which governs the optimal transfer. To verify the predictions, numerical examples are presented.

17. Key Words (Suggested by Author(s)) Orbital Transfer		18. Distribution Statement Unclassified - Unlimited	
19. Security Classif. (of this report) Unclassified	20. Security Classif. (of this page) Unclassified	21. No. of Pages 114	22. Price* $3.00

ACKNOWLEDGEMENT

TABLE OF CONTENTS

LIST OF TABLES

LIST OF ILLUSTRATIONS

NOMENCLATURE

a	semimajor axis, trajectory conic
A	semi-transversal axis, constraining hyperbola
B	semi-conjugate axis, constraining hyperbola
C	center-to-focus distance, constraining hyperbola
C_n	coefficient of the octic equation in V_{C**} ($n = 0$ to 8)
d	perpendicular distance, defined in Fig. 2
e	eccentricity, constraining hyperbola
f	total velocity impulse $= f_1 + f_2$
f_i	velocity impulse at terminal i $= |\Delta\vec{V}_i|$ ($i = 1,2$)
h	angular momentum per unit orbiting mass
k	orbital energy per unit orbiting mass
K	terminal parameter, defined by Eq. (10)
ℓ	distance between two terminal points
M_i, N_i	orthogonal projection of a terminal velocity vector on the V_{Ri} and V_C axes (see Fig. 3)
m_i, n_i	$M_i/\sqrt{\frac{\mu}{r_i}}$, $N_i/\sqrt{\frac{\mu}{r_i}}$
n	terminal distance ratio $= r_2/r_1$
n_c	terminal distance ratio, satisfying the coincidence condition, Eq. 15
P_i	terminal parameter, defined by Eq. (9)
R_n	coefficient of the octic equation in V_{R**} ($n = 0$ to 8)
r	radial distance
$\bar{r}$	semilatus rectum
$\vec{r}$	position vector

S	center-to-vertex distance, evolute Lamé, defined in Fig. C-1
t	time
V	speed
$\vec{V}$	velocity
$\Delta\vec{V}_i$	velocity-increment vector at terminal i, $= |\vec{V}_i - \vec{V}_{01}|$
X	an unspecified trajectory parameter
γ_{Ni}	direction angle of $\Delta\vec{V}_i$ with reference to the normal of transfer plane, defined in Fig. 2
γ_{ri}	direction angle of $\Delta\vec{V}_i$ with reference to local radial direction, defined in Fig. 2
$\gamma_{\theta i}$	direction angle of $\Delta\vec{V}_i$ with reference to local transversal direction, defined in Fig. 2
ϵ	numerical eccentricity, trajectory conic
$\vec{\epsilon}$	eccentricity vector, trajectory conic
θ	true anomaly
μ	gravitational strength of the Newtonian field
ν	nondimensional speed $= V/\sqrt{\frac{\mu}{r}}$
σ	included angle between $\vec{e}_c$ and $\vec{e}_{ri}$ (see Fig. C-1)
σ'	included angle between $\vec{e}_d$ and $\vec{e}_\theta$ (see Fig. C-1)
ϕ	path angle, relative to local horizon
$\mathcal{y}$	base angle, defined in Fig. 1
ψ	central angle, or angle of separation of two terminal position vectors, defined in Fig. 1

Subscripts

0	terminal orbit
1, 2	terminal points
i,j	terminal index
*	stationary 1-impulse solution
**	minimal 2-impulse solution
*j	stationary 1-impulse (at terminal j) solution
i*j	quantity evaluated at terminal i, pertaining to stationary 1-impulse (at terminal j) solution
i**	quantity evaluated at terminal i, pertaining to minimal 2-impulse solution
L, H	low and high trajectories of a bounding pair
C, R	chordal and radial directions
r, θ	radial and transversal directions
P, N	inplane and out-of-plane components
χ, ζ	directions along the interior and exterior base angle bisectors, defined in Fig. 4

Superscripts

$'$	unrealistic
*	critical, or parabolic
T	transpose

Unit Vectors

$\vec{e}_C$	in chordal direction
$\vec{e}_d$	normal to $\vec{e}_C$, in transfer plane
$\vec{e}_N$	normal to transfer plane, defined in Fig. 2
$\vec{e}_{r1}$	$\vec{r}_1/r_1$

$\vec{e}_{r2}$ $-\vec{r}_2/r_2$

$\vec{e}_\theta$ in transversal direction

Special Notations

E   elliptic

H   hyperbolic

P   parabolic

S   simple region, hodograph plane (see Figs. 5 and D-1)

N   nonsimple region, hodograph plane (see Figs. 5 and D-1)

ST   short transfer

LT   long transfer

Q   tip of projection of velocity vector on the transfer plane

Q_{i*} orthopoint, on constraining hyperbola for terminal i

Q_{i*a} orthopoint, corresponding to 1st (absolute) minimal 1-impulse (at terminal i) solution

Q_{i*b} orthopoint, corresponding to maximal 1-impulse (at terminal i) solution

Q_{i*c} orthopoint, corresponding to 2nd minimal 1-impulse (at terminal i) solution

Q_{i*d} orthopoint, corresponding to 3rd minimal 1-impulse (at terminal i) solution

T_{*j} transfer trajectory with stationary impulse at terminal j

T_{*ja} transfer trajectory with absolute minimal impulse at terminal j

T_{*jb} transfer trajectory with maximal impulse at terminal j

T_{*jc} transfer trajectory with 2nd minimal impulse at terminal j

T_{*jd} transfer trajectory with 3rd minimal impulse at terminal j

T_{**} minimal 2-impulse transfer trajectory

I. Introduction

The transfer between two space orbits by applying two terminal impulses under specified terminal conditions is a problem of both theoretical and practical interest in the fuel-optimal space maneuvers. The problem is to determine the optimal transfer trajectory so that the sum of the two terminal impulses is a minimum.

Investigations of the optimal two-impulse orbital transfer problem were first done by Hohmann,[1] and analytical foundations of such investigations were mostly attributed to Lawden's work.[2,10] The 2-terminal, 2-impulse transfer problem, a particular case of Lawden's more general problem, was first formulated and treated by Vargo,[3] and later investigated by many contemporary authors. Among the previous work done on this problem, Altman and Pistiner[12] established an eighth degree polynominal equation governing the optimization, which formed the basis for much of the current development, and a similar equation was also given by Lee.[16] The octic equation was later reformulated in symmetric velocity coordinates and studied under broad terminal conditions by the author.[25] As a result of such investigations, one bewares of the following possible complications in the solution of the problem:

1. The, presence of extraneous roots of the octic equation, which do not belong to the extremal impulse solution.

2. An extremal impulse solution of the octic may give a maximal total impulse instead of a minimal one.

3. There may exist more than one local minimal total impulse solution.

4. The arising of an unrealistic optimal solution, that is, a solution resulting in a transfer trajectory which leads to the final terminal via infinity.

In view of these possible complications, the determination of a realistic absolute minimal 2-impulse solution from the octic equation presents a formidable task, involving many pitfalls, in both theoretical analysis and numerical computations. In the author's previous work, [25] instead of using an algebraic approach to the octic equation, a geometric approach in the velocity space is adopted, and some of the vital questions concerning the solutions were answered, and several necessary or sufficient conditions were derived. Based on this preliminary study, the present paper intends to give a systematic prediction on the characteristics of the minimal 2-impulse solution under various terminal conditions by using the bounding trajectories, a concept first introduced in Ref. [25]. It will be seen that, by the proper choice of a bounding trajectory pair, a great deal of information on the minimal 2-impulse solution, qualitative and quantitative, may be obtained without solving the octic equation, and this information may in turn help to locate the optimal solution in numerical computation.

II. Formulation in Symmetric Velocity Coordinates

Let the terminal conditions be specified by the state coordinates $(\vec{r}_1, \vec{V}_{01})$ and $(\vec{r}_2, \vec{V}_{02})$ at the initial and final terminal points respectively, the problem is to minimize the total velocity impulse

$$f = f_1 + f_2 \tag{1}$$

where

$$f_i = |\overrightarrow{\Delta V_i}| = |\vec{V}_i - \vec{V}_{0i}| \qquad (i = 1,2) \tag{2}$$

and $\vec{V}_i$ is the terminal velocity required for the transfer (Figures 1, 2). Resolving into the oblique velocity components along the terminal radial direction and the chordal direction (Figure 3), Godal's Compatibility conditions[4, 18] enable one to write

$$\vec{V}_1 = V_c \vec{e}_c + V_R \vec{e}_{r1}$$
$$\vec{V}_2 = V_c \vec{e}_c + V_R \vec{e}_{r2} \tag{3}$$

where the velocity coordinates V_C and V_R are connected by

$$V_C V_R = \frac{\mu}{d} \tan \frac{\psi}{2} \tag{4}$$

The central angle ψ and the distance d, as defined in Figure 3 , are completely determined by the position vectors $\vec{r}_1$ and $\vec{r}_2$, which are assumed to be noncollinear, that is, $0 < \psi < \pi$. The coordinate pair (V_C, V_R) is known as the symmetric velocity coordinate pair in view of Equations (3).

3
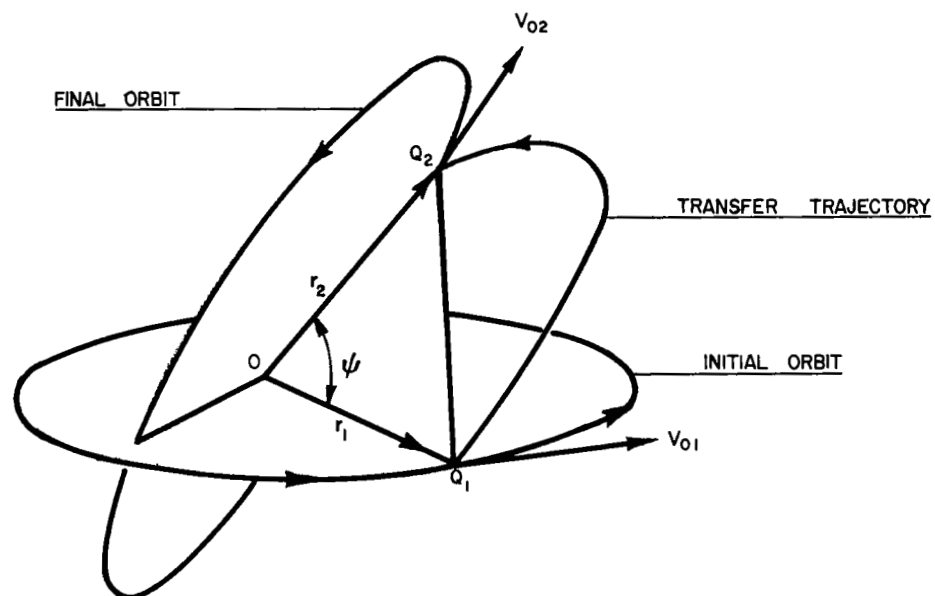
FIG. 1   GEOMETRY OF 2-TERMINAL TRANSFER IN SPACE
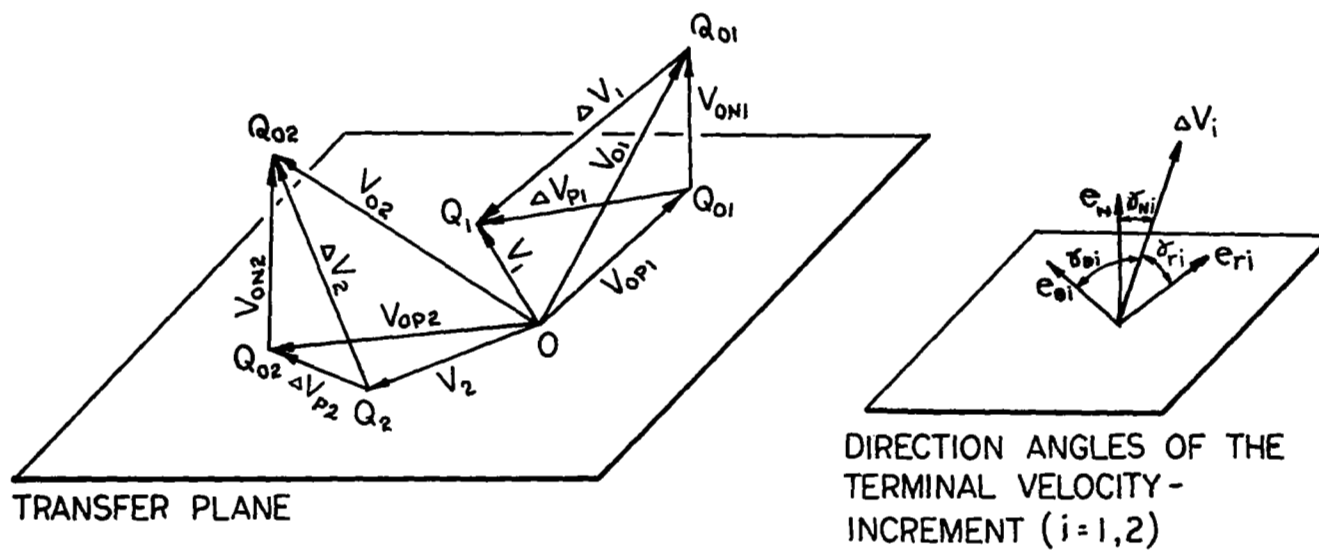
FIG. 2   GEOMETRY OF VELOCITY VECTORS,   2-IMPULSE TRANSFER
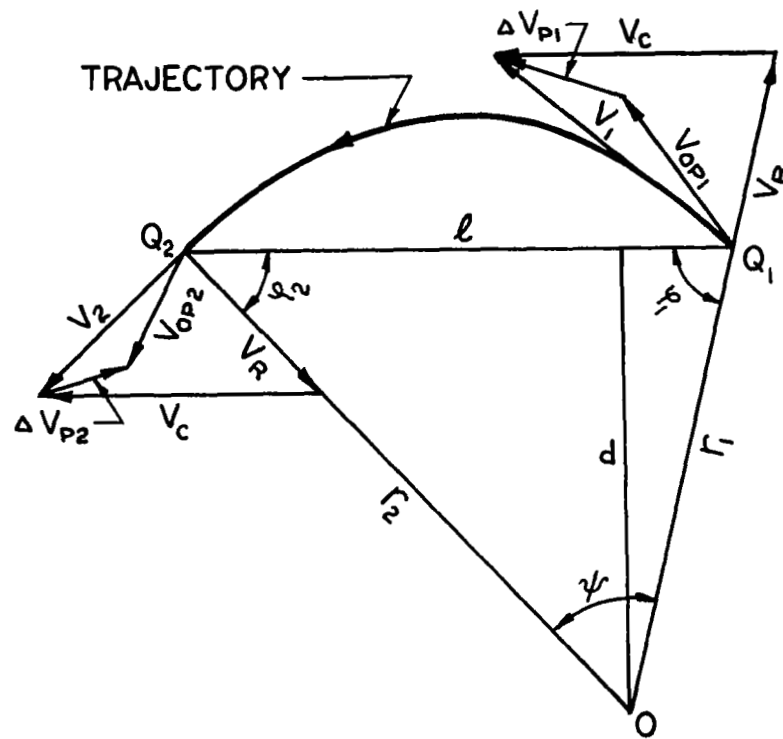
TRAJECTORY

THE TRANSFER TRAJECTORY
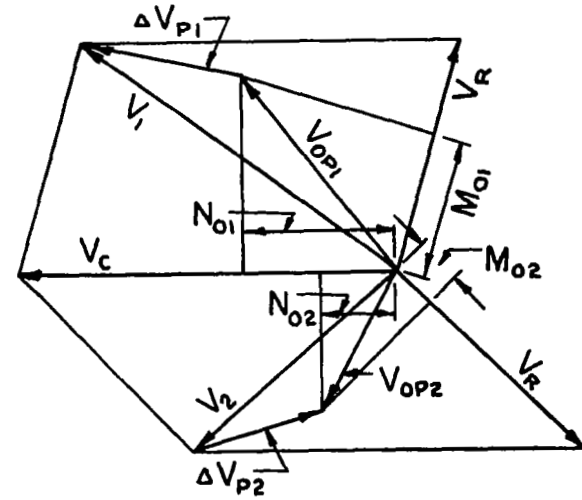
THE IN-PLACE VELOCITY COMPONENTS
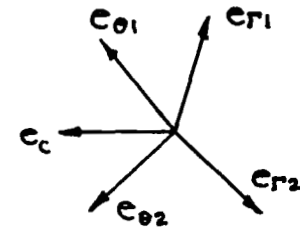
THE REFERANCE UNIT VECTORS

FIG. 3 THE TRANSFER TRAJECTORY AND THE IN-PLANE VELOCITY COMPONENTS

and (4) which hold for all transfer trajectories between the two terminal points.

The analytic condition governing the optimal transfer is given by

$$df_1 + df_2 = 0 \tag{5}$$

which, after performing the differentiation together with Equations (2), (3) and (4), yields the two polynomial equations, known as the stationarity octics[25],

$$\sum_{n=0}^{8} C_n v_{c**}^n = 0 \tag{6c}$$

$$\sum_{n=0}^{8} R_n v_{R**}^n = 0 \tag{6R}$$

where the coefficients C_n and R_n are functions of the following terminal parameters:

$$M_{0i} = \vec{V}_{0i} \cdot \vec{e}_{ri} \tag{7}$$

$$N_{0i} = \vec{V}_{0i} \cdot \vec{e}_c \tag{8}$$

$$(i = 1, 2)$$

$$P_{0i} = V_{0i}^2 - 2K \cos \varphi_i \tag{9}$$

$$K = \frac{\mu}{d} \tan \frac{\psi}{2} \tag{10}$$

Thus we may write

$$C_n = C_n(M_{01}, M_{02}, N_{01}, N_{02}, P_{01}, P_{02}, K)$$

$$R_n = R_n(M_{01}, M_{02}, N_{01}, N_{02}, P_{01}, P_{02}, K) \tag{11}$$

For fixed terminal conditions all these coefficients are constants, and Equations (6C) and (6R) define a pair of optimal

values of V_{C**} and V_{R**} for an internal extremum of f. Derivations of the stationarity octics and the explicit forms of Equations (11) are given in Appendix A, and formulas for the transfer trajectory parameters in terms of the symmetric velocity coordinates V_C and V_R are summarized in Appendix B.

As shown in Reference 25, the minimal 2-impulse transfer trajectory T_{**}, defined by Equation (5), is bounded between the two transfer trajectories, T_{*1} and T_{*2}, defined by

$$df_1 = 0 \quad \text{and} \quad df_2 = 0 \tag{12}$$

respectively. In terms of the coordinate V_C, Equation (12), together with the constraint Equation (4), yields the two fourth degree equations

$$V_{C*1}^4 - N_{01}V_{C*1}^3 + KM_{01}V_{C*1} - K^2 = 0 \tag{13C-1}$$

$$V_{C*2}^4 - N_{02}V_{C*2}^3 + KM_{02}V_{C*2} - K^2 = 0 \tag{13C-2}$$

known as the stationarity quartics[20], one for each terminal. Similar equations may be written in terms of the variables V_{R*1} and V_{R*2}. The trajectories T_{*1} and T_{*2}, defined by Equations (13C-1, 2), have the physical significance of being the transfer trajectories between the same two terminal points Q_1 and Q_2, with stationary velocity impulses at Q_1 and Q_2 respectively, hence they will be referred to as the stationary 1-impulse transfer trajectories. Analytic studies of Equations (13C-1, 2)[20] show that each quartic has at least two and at most four

real roots, depending on the terminal conditions. In other words, each stationarity quartic may yield two to four distinct stationary 1-impulse transfer trajectories. The choice of such trajectories for the bounding pair will be postponed until the transfer geometry in the velocity space is studied.

III. Preliminaries on the Two-Terminal Transfer

Based on the geometric studies of two-terminal transfers in the position and velocity spaces,[18, 20, 25] some previously developed concepts and terminology which form the background of the present investigation will now be briefly given below.

A. On the Constraining Hyperbola

1. The tip of the transfer velocity vector at each terminal required for a 2-terminal transfer, is confined in the hodograph plane on a hyperbola, defined by Godal's compatibility condition, Eq. (4). Such a hyperbola is called the constraining hyperbola for the terminal velocity, and there is one for each terminal. The geometry of each constraining hyperbola is completely determined by the two position vectors $\vec{r}_1$ and $\vec{r}_2$. Characteristics of the constraining hyperbola, and its principal geometric elements are summarized in Appendix C.

2. Each constraining hyperbola consists of two branches:

the positive branch: $V_C > 0$, $V_R > 0$, associated with short transfers;

the negative branch: $V_C < 0$, $V_R < 0$, associated with long transfers.

The positive branches of the two constraining hyperbolas constitute a short transfer pair, while the two negative branches, a long transfer pair (See Figure 4). The half-plane ($V_\zeta > 0$) in which the positive branch lies will be designated as the positive half-plane, and that ($V_\zeta < 0$) in which the negative branch lies, the negative half-plane.

3. All solution points in the hodograph plane for the two-terminal transfers, optimal or nonoptimal, are necessarily confined on the constraining hyperbolas. The solution point (Q_1) for the initial terminal velocity and its corresponding point (Q_2) for the final terminal velocity form a pair of transfer points. The line connecting a transfer point pair bisects the angle of separation ψ.[4, 18]

4. The type of the transfer conic will be elliptic, hyperbolic, or parabolic according as the transfer point Q_i lies inside, outside, or on the critical circle, $V = V^*$, in the hodograph plane. Thus, each branch of the constraining hyperbola is divided by the critical circle into two portions: the elliptic portion and the hyperbolic portion as shown in Figure C-1, Appendix C. The points of intersection of the hyperbola and the critical circle are the critical points corresponding to parabolic transfers. The hyperbolic portion, including its end point, the critical point, in the half-plane, $V_\chi > 0$, is the unrealistic portion since it corresponds to unrealistic transfer trajectories.[20]
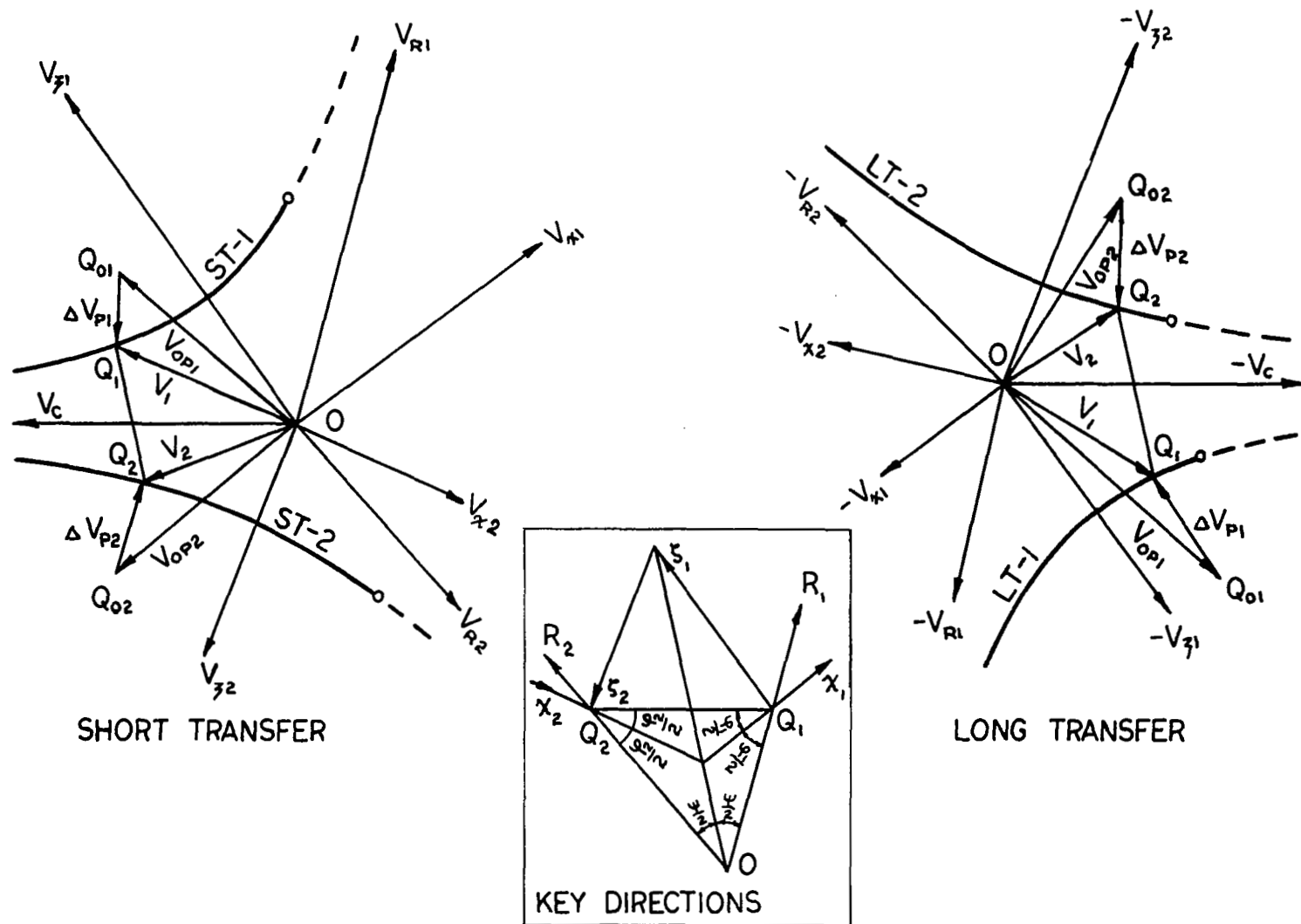
FIG. 4 THE TRANSFER PAIR OF CONSTRAINING HYPERBOLAS

B. On the Stationary One-Impulse Transfer and the Orthopoints

   1. Geometrically, the stationarity quartic, based on Equations (12) expresses the condition of orthogonality[8,20]

$$\Delta \vec{V}_i \cdot \vec{dv}_i = 0 \tag{14}$$

It follows that, when a terminal velocity $\vec{V}_{0i}$ is prescribed, each solution point for the stationary one-impulse transfer is given by the foot of the normal drawn from the point Q_{0i}, the projection of the tip of V_{0i} in the hodograph plane, to the constraining hyperbola. Such a point is called the orthopoint with respect to the fixed point Q_{0i}, and is designated as Q_{i*}. Hence each real root of the stationarity quartic corresponds to one orthopoint on the constraining hyperbola, and vice versa.

   2. As each stationarity quartic may have two to four real roots, the number of orthopoints for a given terminal velocity point Q_{0i} range from two to four. Previous studies[20] show that these orthopoints follow a general pattern as follows:

Orthopoint Designation	Nature of f_i
Q_{i*a}	1st minimum, absolute.
Q_{i*b}	maximum.
Q_{i*c}	2nd minimum, local.
Q_{i*d}	3rd minimum, local.

Here the points Q_{i*b} and Q_{i*c} may be coinciding or missing in the real plane, depending on the location of Q_{0i}. We may speak of the orthopoint as elliptic, parabolic, or hyperbolic, and realistic or unrealistic, according to the nature of the portion of the constraining hyperbola on which it locates.

3. The hodograph plane may be divided into different regions for the terminal velocity point Q_{0i} according to the number and nature of the orthopoints associated with it (See Figure 5).

The simple and nonsimple regions are separated by the evolute of the constraining hyperbola, which is a form of Lamé[20] as follows:

Region	Designation	Orthopoints
Simple	S	2, one on each branch.
Nonsimple	N	4, three on the nearer branch (Q_{i*a}, Q_{i*b}, Q_{i*c}), and one on the other (Q_{i*d})

On the boundary two of the three points on the same branch coincide, $Q_{i*b} = Q_{i*c}$, where f_i is neither minimum nor maximum; and at each vertex of the boundary, all three points on the same branch, Q_{i*a}, Q_{i*b} and Q_{i*c} coincide, with absolute minimum f_i. Typical distributions of the orthopoints are shown in Figure D-1, Appendix D (where the terminal subscript i has been omitted for simplicity).
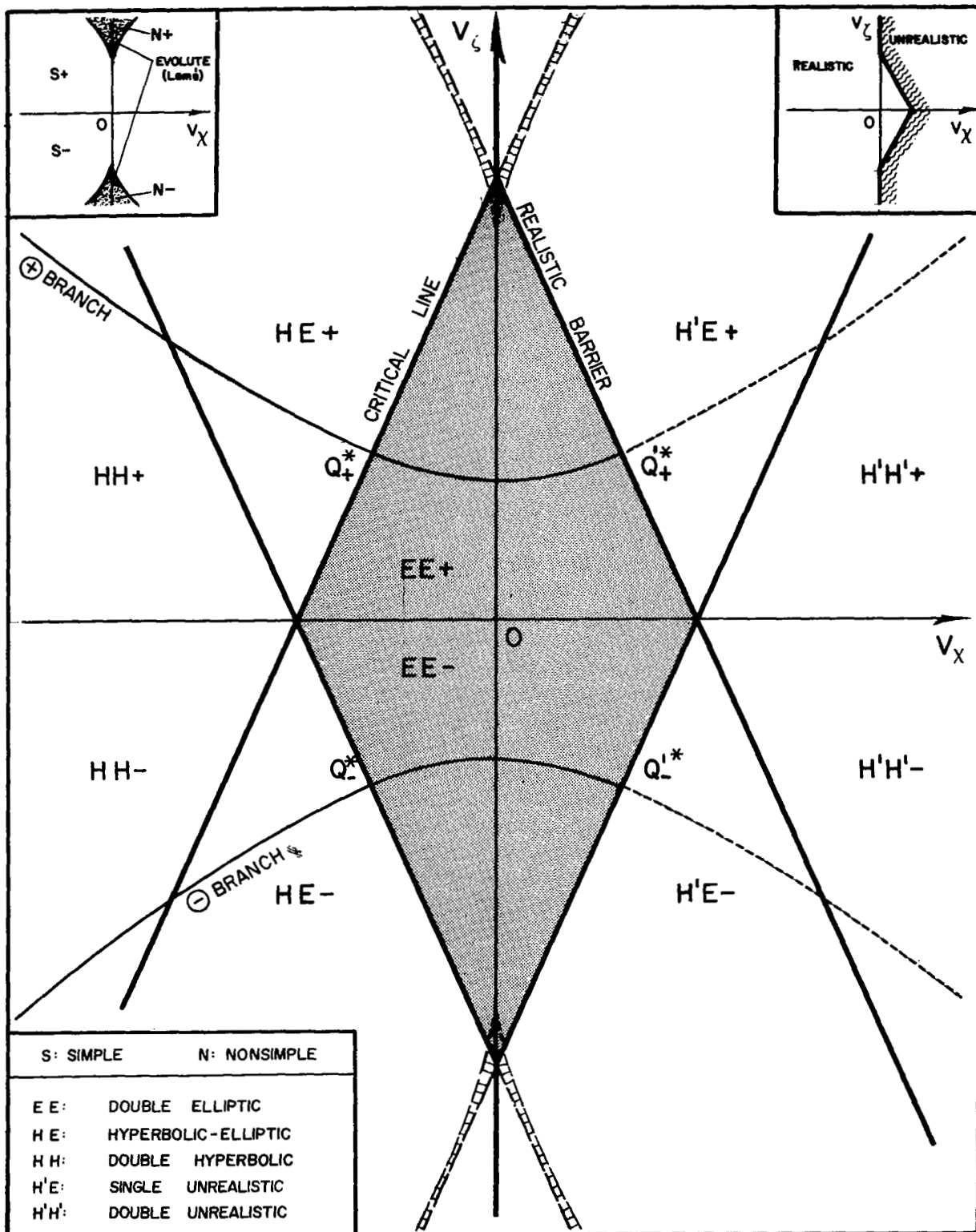
FIG. 5   THE HODOGRAPH REGION DIAGRAM

The realistic and unrealistic regions are partitioned according as the first minimal point, (Q_{i*a}), hence its associated trajectory, is realistic or unrealistic, as shown in Figure 5. The bounding lines consist of the critical lines, which are the normal lines through the critical points in the half-plane $V_\chi > 0$, and portions of the V_ζ - axis.

The realistic region may be further divided into a number of subregions for the point Q_{0i} according to the types of the trajectories associated with the orthopoints as follows:

Subregion	Designation
Double Elliptic	EE
Hyperbolic-Elliptic	HE
Double Hyperbolic	HH

Here the first letter indicates the type of the trajectory associated with Q_{i*a}, and the second letter, that associated with Q_{i*d}. The points Q_{i*b} and Q_{i*c}, if they exist, and their associated trajectories will be of the same type as that of Q_{i*a}, or Q_{i*d}. On the critical lines, at least one of the trajectories is parabolic.

Likewise, the unrealistic region may be further divided as follows:

Subregion	Designation
Single Unrealistic	H'E
Double Unrealistic	H'H'

Here the same convention of designations used for the realistic subregions is adopted, with the superscript ' indicates unrealistic transfer.

All the foregoing divisions of hodographic regions apply, of course, to either terminal point. For details, see Appendix D.

IV. The Bounding Trajectories for the Minimal
Two-Impulse Transfer

A. The Optimal Transfer Arc Pair

Assume the terminal velocity point Q_{0i} is fixed, and
let the transfer point Q_i move along the constraining
hyperbola. For convenience we designate the hyperbolic arc
as positive or negative according as the distance $\overline{Q_{0i}Q_i}$ ($=f_i$)
is increasing or decreasing as Q_i moves from left to right.
Evidently, the arc will change sign only when Q_i passes
through an orthopoint. The stationarity condition expressed
by Equation (5) indicates clearly that the two-impulse
optimal solution must locate on a transfer pair of arcs of
opposite signs. The essential types of such arc pairs are
shown in Figure 6.

In type (A) the endpoints of the arc pair are the
minimal orthopoints, one on each arc, together with their
cotrajectory points. They may be either Q_{i*a}, Q_{i*c}, or
Q_{i*d}. It is assumed that no other orthopoints exist on
either arc between its endpoints. On such an arc pair
there is one and only one local minimal solution.[†]

Type (B) is a variation of type (A). It contains a
maximal orthopoint on one of the arcs between its
endpoints. Analytic studies show that there is either
one local minimal solution and one local maximal solution
on the arc pair, or none.[†] If such solutions exist, they

[†] See Appendix E

19

(A)　(B)　(C)　(D)

$Q_{*1 MIN}$　$Q_{*1 MAX}$　$Q_{*1 MIN}$　$Q_{*1 MAX.}$

$+$　$+$　$+$　$-$

$-$　$-$　$-$　$+$

$Q_{*2 MIN}$　$Q_{*2 MIN}$　Q'^{*}_{2}　$Q_{*2 MIN}$　$Q_{*2 MAX.}$

ONE LOCAL MIN.　ONE LOCAL MIN. AND ONE LOCAL MAX, OR NONE.　ONE LOCAL MIN, (REALISTIC OR UNREALISTIC.)　ONE LOCAL MAX.
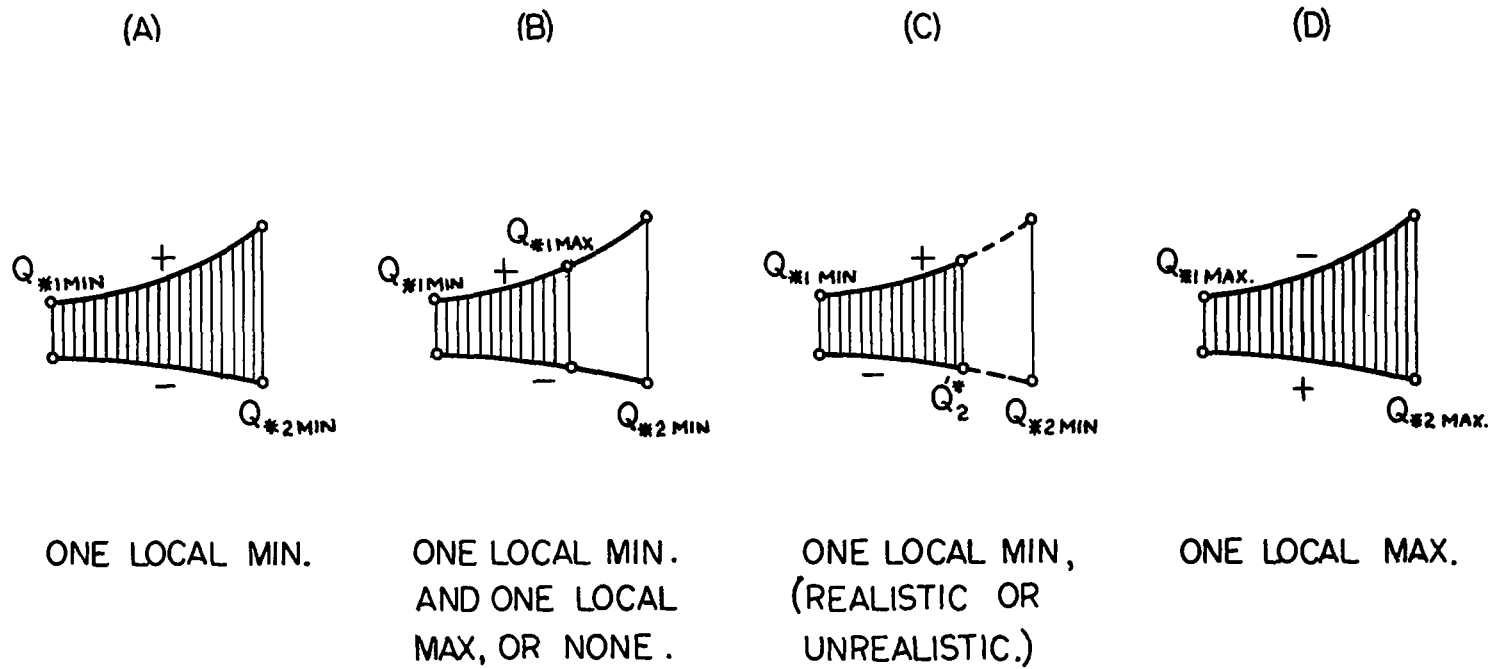
FIG. 6　TYPICAL PAIRS OF THE OPTIMAL TRANSFER ARCS

will actually locate on the subarc pairs defined by the two orthopoints, one minimal and one maximal, on the same arc.

Type (C) is another version of type (A), wherein one of the minimal orthopoints is unrealistic, and the arc pair is defined on the righthand side (Figure 6) by the unrealistic critical point pair. The two-impulse minimum then may be either realistic or unrealistic. In the latter case the realistic optimal solution will be indefinite, given by an arbitrary point pair on the arc pair, close to the unrealistic critical point pair.[20]

In type (D) the arc pair is defined by the maximal orthopoints, one on each arc, together with their cotrajectory points. It contains one maximal solution only, but no minimal solution.[†]

Thus, in order to locate the two-impulse minimal solution it is only the arc pairs of type (A) and its two variations (B) and (C) which need to be examined. The exclusion of the arcs of the same sign automatically prevents the entering of the extraneous roots of the stationarity octic, if any; and the exclusion of the arc pair of type (D) further prevents the entering of the maximal solution. Consequently the problem narrows down to searching the absolute minimal solution on the arc pairs of types (A), (B), and (C), where the local minimal solutions are located.

[†]See Appendix E

Since each optimal arc pair is essentially defined by two orthopoints, one at each end, together with their cotrajectory points, we may specify such an arc pair by giving the two orthopoints as its coordinates, e.g., (Q_{1*a}, Q_{2*d}) is a typical optimal arc pair, which may also be written more compactly as (a, d). By ignoring the order of the terminal points, we may regard the arc pairs (a, d) and (d, a) as of the same combination (ad). Evidently, optimal arc pairs of the basic types (A) may have the following six combinations:

(aa), (ad), (dd), (ca), (cc), (cd).

By associating b with one of the endpoints, a or c, we obtain the combinations for the arc pairs of the type (B). There are also six such combination; namely,

(ab-a), (ab-c), (ab-d), (cb-a), (cb-c), (cb-d).

Arc pairs of type (B) and the last three combinations of type (A) would not be possible unless one or both of the terminal velocity points, Q_{01} and Q_{02} are in the nonsimple regions, of course. By replacing any one of the orthopoints by an unrealistic critical points as one endpoint, we obtain the optimal arc pairs of type (C).

As regards to the selection of the optimal arc pair for the absolute minimum, no rigorous rules are available at present. However, the following observations may serve as a guide:

1. When an optimal arc pair of the combination (aa) appears, the two absolute 2-impulse minimum are most likely on that pair.

2. The local minimum provided by the arc pair (dd) is usually not absolute.

Thus, to locate the absolute 2-impulse minimum we first look for the arc pair (aa). The arc pair (dd), if it exists, may usually be ignored. In the absence of arc pairs of the combination (aa) and (dd), or there is any doubt, one may always resort to the computation of all the local minimal solutions and comparision, of course.

B.   The Bounding Trajectory Pair

Associated with each optimal arc pair there are two transfer trajectories, one corresponding to each endpoint pair. The existence of an interior minimum for the two-impulse transfer on such an arc pair shows that the minimal two-impulse transfer trajectory, denoted by T_{**}, is actually bounded between the two bounding trajectories, hence the term "bounding trajectory pair". It will be shown that T_{**} is not only bounded by such a trajectory pair in the position space, but also in the velocity space and many other parameter spaces. Thus essential information on the characteristics of the two-impulse minimum may be obtained by examining its bounding trajectory pair.

Since an endpoint pair of the optimal arc pair consist of basically one orthopoint and its cotrajectory point, a

bounding trajectory is in general a stationary trajectory
with respect to the velocity impulse at one of the terminals.
In the special case wherein one of the endpoint pair is
critical and unrealistic, the corresponding trajectory is
the unrealistic parabola, which itself is unbounded in the
position space; nevertheless, it may serve as a bounding
trajectory. Designations of the bounding trajectories are
made in accordance with the endpoints they associate with
as follows:

Endpoint	Bounding Trajectory
Q_{i*a}	T_{*ia} , 1st minimal (abs.) one-impulse transfer
Q_{i*b}	T_{*ib} , maximal one-impulse transfer
Q_{i*c}	T_{*ic} , 2nd minimal one-impulse transfer
Q_{i*d}	T_{*id} , 3rd minimal one-impulse transfer
Q_{i*}'	$T_{*i}^{*'}$, unrealistic parabolic transfer

With this designation convention the coordinates specifying
an optimal arc pair may now be extended to a bounding
trajectory pair. For example, corresponding to the arc
pair (a,d), we have the bounding trajectory pair (T_{*1a}, T_{*2d}).
Consequently, the different combinations previously given
for the optimal arc pairs also apply to the bounding
trajectory pairs. Thus corresponding to the six possible
combinations for the arc pairs of type (A), there are six
possible combinations of the bounding trajectory pair.
The same can be said about the bounding trajectory pairs
associated with the arc pairs of types (B) and (C).

Directly from the previous analysis of the optimal transfer arc pairs, the following observations may now be made:

1. Basically, a bounding trajectory pair is formed by two transfer trajectories under the same terminal conditions, one with a minimal initial velocity impulse, and the other with a minimal final velocity impulse. (Such a trajectory pair will be generally denoted by (T_{*1}, T_{*2}). Subscripts will be added in accordance with the endpoints of the associated transfer arc pair whenever necessary.)

2. A bounding trajectory pair associated with the optimal transfer arc pair of type (A) will bound one and only one local minimal two-impulse transfer trajectory between them; and, in particular,

   (a) A bounding pair (T_{*1a}, T_{*2a}) formed by the two first minimal (absolute) one-impulse transfer trajectories with respect to the initial and final velocity impulses separately usually bounds the absolute minimal two-impulse transfer trajectory;

   (b) A bounding trajectory pair (T_{*1d}, T_{*2d}) formed by the two third minimal one-impulse transfer trajectories with respect to the initial and final velocity impulses separately bounds only a local minimal two-impulse transfer trajectory which is usually not the absolute one.

2. When the optimal arc pair is of the type (B), the bounding pair made of the two minimal one-impulse transfer trajectories may bound one local minimal two-impulse transfer

trajectory, or none. If it does bound one, then there exists
a closer bounding pair formed by the two transfer traject-
ories, one with a minimal velocity impulse, and the other with
a maximal velocity impulse, both at the same terminal, e.g. (T_{*1a}, T_{*1b}).

3. When one of the bounding trajectories is unrealistic
(optimal arc pairs of type (C)), the minimal two-impulse
trajectory bounded may become indefinite.

Several typical bounding trajectory pairs are
illustrated in Figure 7.

It is to be noted that although there appears to be a
great variety of the optimal transfer arc pairs and their
associated bounding trajectory pairs, they do not all occur
frequently. For example, when both terminal velocity points,
Q_{01} and Q_{02}, are in the realistic simple regions, as is
usually the case. The pattern of the optimal arc pairs can
fall under the following two classes only:

Class	One Kind of Transfer	Other Kind of Transfer
I	(a, a)	(d, d)
II	(a, d)	(d, a)

In Class I the absolute minimal two-impulse transfer trajectory
will likely be bounded by the trajectory pair (T_{*1a}, T_{*2a}),
but unlikely by the pair (T_{*1d}, T_{*2d}). Hence in this case
it is only to the former pair our attention is to be focused.
In Class II each of the bounding pairs (T_{*1a}, T_{*2d}) and
(T_{*1d}, T_{*2a}), one in each kind of transfer, bounds a local
minimal two-impulse transfer trajectory in that kind, and
in the search of an absolute minimum, the consideration of
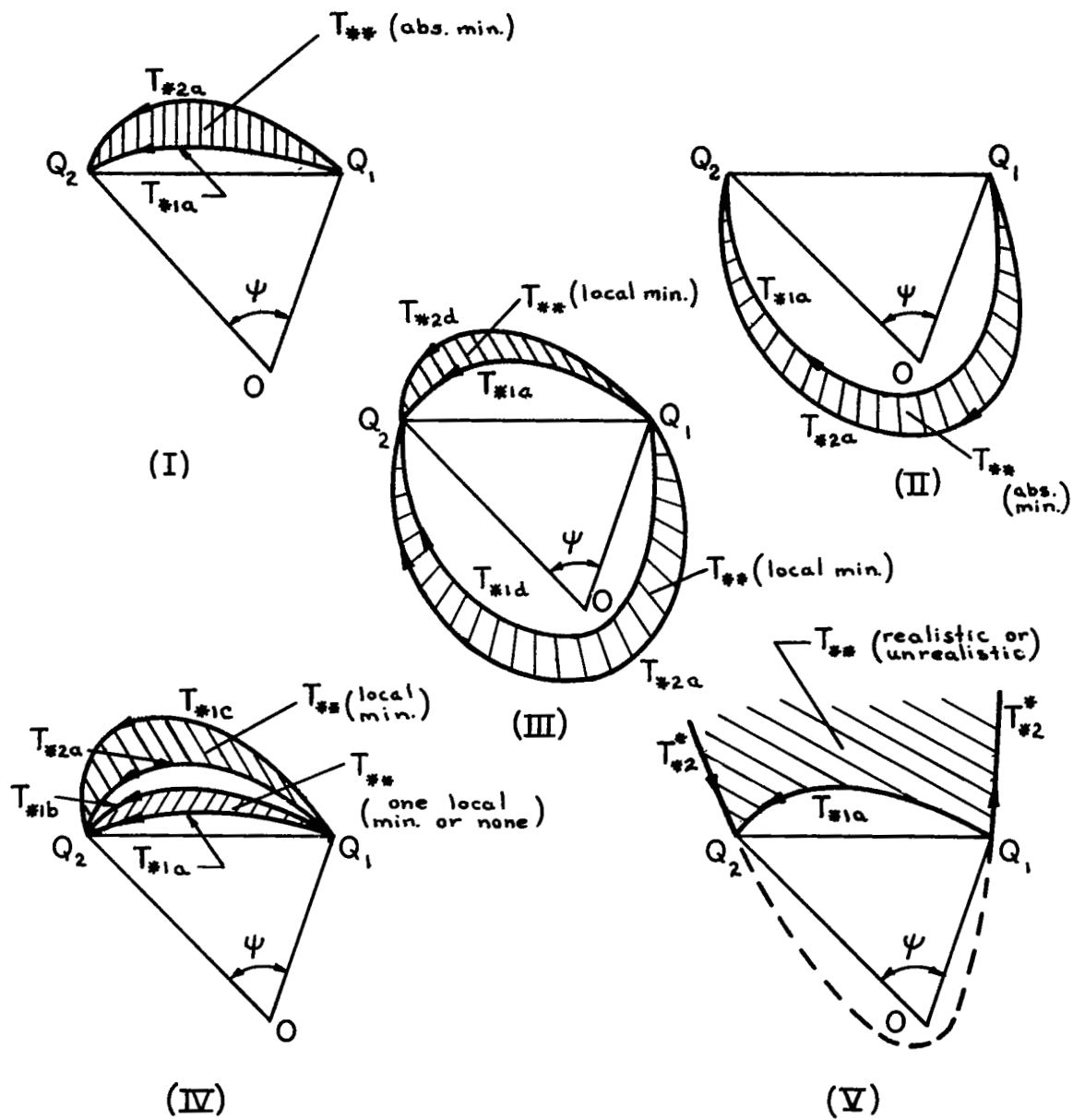
FIG. 7 TYPICAL PAIRS OF BOUNDING TRAJECTORIES

27

of both kinds is then necessary. In either case the number of bounding pairs to be considered is no more than two. Real complications can arise only when one or both of Q_{01} and Q_{02} are in the nonsimple and/or unrealistic regions, wherein more types of the optimal arc pairs may appear, and more bounding trajectory pairs are to be considered. Further discussions will be found in the next section.

V.   Qualitative Predictions on the Minimal Two-Impulse
     Transfer

A.   The Kind and Sense of the Transfer

For the transfer between two terminal points separated
by a central angle $0 < \Psi < \pi$, there is a definite sense of
motion around the field center, associated with each kind
of transfer. In the following we will arbitrarily assign
a positive sense to the short transfer, and a negative
sense to the long transfer. It is clear that the two
trajectories of a bounding pair (T_{*1}, T_{*2}), as defined in
the preceding section, are of the same kind and sense, and
so is the minimal two-impulse trajectory T_{**} bounded between
them. Thus, whenever a bounding trajectory pair is given,
the kind and, hence, the sense of the minimal two-impulse
trajectory bounded is fixed. Obviously the kind and sense
of a bounding trajectory pair depend only on those of the
optimal arc pair, but not on the particular endpoints
defining it.

As pointed out in Reference 25, it is interesting to
note that, while the sense of the minimal two-impulse
transfer always agree with those of the two bounding
trajectories, it does not necessarily agree with those of
the two terminal orbits even though they have the same sense.[†]

[†]When the two terminal orbits are noncoplanar, it is
to be understood that the sense of motion of each orbit
refer to that of the projection of the orbit on the transfer
plane.

This peculiar phenomenon stems from the fact that the
stationary one-impulse transfer trajectory does not always
agree in sense with the corresponding terminal orbit. The
particular case in which two terminal orbits of the same
sense call for a minimal two-impulse transfer in the opposite
sense is illustrated in Reference 25.

B. Type of the Transfer Conic

A study of the hodograph geometry enables one to
establish the following rules for determining the type of
the minimal two-impulse transfer conic in terms of the
bounding trajectories:

1. T_{**} will be elliptic if at least one of T_{*1} and T_{*2}
is elliptic, and none of them is hyperbolic;

2. T_{**} will be hyperbolic if at least one of T_{*1} and
T_{*2} is hyperbolic, and none of them is elliptic;

3. T_{**} will be parabolic if both T_{*1} and T_{*2} are
parabolic.

Thus, once the bounding trajectory pair is chosen, the type
of the minimal two-impulse transfer conic is uniquely
determined under the foregoing three conditions. The only
ambiguous case is that the bounding trajectory pair consists
of one ellipse and one hyperbola, wherein the type of T_{**}
is indeterminate.

The type of each bounding trajectory, T_{*i}, is of course,
determined by the terminal conditions. Once the terminal
point Q_{0i} is located in the hodograph plane, the region

diagrams illustrated in Figure 5 will enable one to tell immediately the type of T_{*i}.

Finally, it is to be mentioned that, while the two-impulse minimum always agrees in type with its two bounding trajectories of the same type, it is not necessarily so with the two terminal orbits of the same type. Just like in the case of kind and sense, this stems from the fact that a one-impulse minimal transfer trajectory does not always agree in type with the corresponding terminal orbit, a situation found in Reference 20. Thus, for minimal total impulse, it is possible that two elliptic orbits call for an hyperbolic transfer; and that two hyperbolic orbits, an elliptic transfer.

C.   The Realistic and the Unrealistic Transfers

Concerning the nature of the minimal two-impulse transfer, realistic or unrealistic, the following criteria are evident:

1. T_{**} will be realistic if both T_{*1} and T_{*2} are realistic;

2. T_{**} will be unrealistic if both T_{*1} and T_{*2} are unrealistic.

Thus once a bounding trajectory pair is found, the nature of T_{**} is determined, unless the bounding pair consists of one realistic and one unrealistic, wherein the nature of T_{**} is not ascertained. The optimal transfer arc pair under Condition 2 actually reduces to one point pair--the

31

unrealistic critical one; and the two bounding trajectores, T_{*1} and T_{*2}, both coinciding with the unrealistic parabolic trajectory.

It is to be noted that, while the two-impulse minimum in one kind of transfer is unrealistic, there may exist a realistic minimum in the other kind. Thus, it is sometimes advisable to examine the bounding trajectory pairs in both kinds. This is necessary when the two first minimal one-impulse transfer trajectories, T_{*1a} and T_{*2a}, are of unlike kinds, for example, the condition under Class II, Section IV-B (last paragraph). In such a case it is quite possible to have one realistic absolute minimum in one kind, and one unrealistic local minimum in the other. The foregoing criteria apply to either kind, of course.

Obviously, the nature of each bounding trajectory is determined by the terminal conditions. For two fixed terminal points, such a determination may be readily made by using the hodographic region diagram in Figure 5 once the terminal velocity point Q_{01} is located. It is clear from such diagrams that Condition 1 is satisfied for both kinds when Q_{01} and Q_{02} are both in their realistic regions; and Condition 2 is satisfied for both kinds when they are both in their double unrealistic regions. In the latter case, there exists no realistic absolute minimum solution of the problem, and the solutions in both kinds are indefinite.

D. The Multiplicity of the Minimal Solutions

By multi-minimum we mean distinct transfer trajectories giving the same local minimal total impulse f_{**} under the same terminal conditions. Evidently, no multi-minimum in the same kind of transfer can be expected unless there are multiple pairs of bounding trajectories in the same kind for choice, corresponding to the multiple optimal transfer arc pairs of that kind. Thus, a pre-requisite for the occurrence of a multi-minimum of one kind is that at least one of the terminal velocity points, Q_{01} and Q_{02}, is in its nonsimple region. Although there are six combinations for the optimal arc pairs of the basic type, as given in Section IV-A, studies of the distributions of the orthopoints in the constraining hyperbola show that there can be no more than three different arc pairs of the same kind. Consequently, no multiplicity higher than three can be expected for the same kind of transfer. Details of such studies are given in Appendix F, from which the following assertions may be made:

Concerning Multi-Minimum of the Same Kind.

1. No multi-minimum may arise when both terminal velocity points are in their simple regions.

2. When one and only one of the terminal velocity points is in its nonsimple region, there exists at most a double minimum.

3. No triple minimum can be expected unless both terminal velocity points are in their nonsimple regions.

4. No multiplicity higher than three can be expected under any terminal conditions.

The actual existence of a double minimum of the same kind has been illustrated in Reference 25. However, whether a triple minimum of the same kind actually exist has not been ascertained. A proof of its existence or nonexistence would be of theoretical interest.

Now considering both kinds of transfers, it is evident that a double minimum is possible even when both terminal velocity points are in their simple regions, since there is one local minimum in each kind in this case. Maximum multiplicity will be higher when one or both of the terminal velocity points are in their nonsimple regions. However, as shown in Appendix F, the total number of optimal arc pairs of both kinds cannot exceed four under any fixed terminal conditions. Thus a quadruple minimum of mixed kinds can be expected at most. A study of Appendix F enables one to further assert the following:

Concerning Multi-Minimum of Mixed Kinds

1. When both terminal velocity points are in their simple regions, there exists at most a double minimum.

2. When one and only one of the terminal velocity points is in its nonsimple region, there exists at most a triple minimum.

3. When both terminal velocity points are in their nonsimple regions, there exists at most a quadruple minimum.

4. No multiplicity higher than 4 can be expected under any terminal conditions.

As example of a quadruple minimum, consisting of two double minimal, one in each kind, all with the same minimal f_{**}, is shown in Reference 25.

E. The Identical Minimal Two-Impulse and Minimal One-Impulse Solutions

It is obvious that when the two trajectories of a bounding pair becomes coincident, the two-impulse minimal transfer trajectory bounded between will necessarily coincide with them, that is,

$$T_{**} = T_{*1} = T_{*2}$$

Thus, the minimal two-impulse solution will be identical to the two minimal one-impulse solutions, one with respect to the initial terminal impulse, and the other, the final terminal impulse, when they themselves are identical. This can also be easily seen by referring to the basic governing equations (5) and (12). In fact, the simultaneous validity of any two of the three equations assures the validity of the third one. Thus we conclude:

The coincidence of any two of the three trajectories,

T_{*1}, T_{*2} and T_{**} implies the coincidence of all three. The optimal transfer arc pair now actually reduces to merely

a transfer point pair. The unrealistic case mentioned under Heading C offers a special example of this case.

An analytic condition for the occurrence of such identical solutions, as deduced in Reference 25, is

$$K[(M_{02}-M_{01})^2-(N_{02}-N_{01})^2]^2 = (M_{02}-M_{01})(N_{02}-N_{01})$$
$$(M_{02}N_{01}-M_{01}N_{02})^2 \qquad (15)$$

which may be written symbolically

$$F(\vec{r}_1,\vec{r}_2,\vec{V}_{01},\vec{V}_{02}) = 0 \qquad (16)$$

Thus there is a definite relation to be satisfied by the four terminal vectors, $\vec{r}_1,\vec{r}_2,\vec{V}_{01}$ and $\vec{V}_{02}$ in order that the two-impulse minimization and the one-impulse minimizations at the initial and the final terminals separately will yield the same trajectory. Such a relation will be referred to as the coincidence condition for the two-impulse minimization and the two one-impulse minizations for the two-terminal transfer. It can be shown that the condition given by Equation (15) is not only necessary, but also sufficient. It is interesting to note that Equation (15) is, in particular, satisfied by

$$M_{01} = M_{02} \quad \text{and} \quad N_{01} = N_{02} \qquad (17)$$

In the case of apside-to-apside transfer, $M_{01} = M_{02} = 0$, Equation (17) lead to

$$\frac{V_{op^2}}{V_{op^1}} = \frac{r_2}{r_1} \qquad (18)$$

Thus, a sufficient condition for the coincidence of T_{*1}, T_{*2} and T_{**} is that the base triangle determined by the two

position vectors, and the velocity triangle determined by the two in-plane terminal orbit velocities are similar and orthogonal.

Finally, it is to be noted that, in the previous assertion on the coincidence of the three transfer trajectories, T_{*1}, T_{*2} and T_{**}, it has been tacitly assumed that the two terminal impulse functions, f_1 and f_2, are both differentiable. This assertion and the coincidence condition, Equation (15) all break down when f_1' and f_2' do not both exist. Such a case may be called singular. In a singular case, it is possible to have T_{**} coincident with one of T_{*1} and T_{*2}, which do not themselves coincide. The special case wherein one of the terminal orbits passes through both terminal points, is a singular one. For example, if the initial terminal orbit also passes through the final terminal point, then this orbit itself is T_{*1}, and we may have $T_{**} = T_{*1} \neq T_{*2}$.

VI. Quantitative Predictions on the Minimal Two-Impulse Transfer

So far the predictions have been made on the qualitative basis. Quantitative predictions on the various trajectory variables and elements are now in order. In the following, the upper and lower bounds of these trajectory quantities will be established by using the bounding trajectory pair.

A. The Position Vector

Consider a pair of trajectories in a two-terminal Keplerian trajectory family. It is obvious that the one with a higher initial path angle (with reference to the local transverse direction) will remain higher in radial distance on any intermediate radius vector throughout the trajectory range; for, otherwise, the two trajectories will intersect at least at one intermediate point between the two common terminal points, a fact impossible for two distinct Keplerian conics. Such an observation enables one to classify a pair of bounding trajectories as high and low, and indicate them by the subscripts H and L respectively. Thus, instead of T_{*1} and T_{*2}, we write T_{*L} and T_{*H}. Quantities pertaining to the high, or the low trajectory may be indicated in the same way. Such notations will be employed in the following formulations whenever it is convenient.

The existence of an interior point pair on an optimal transfer arc pair for the minimal two-impulse solution (see Section IV and Appendix E) implies that such a minimal trajectory is bounded between the two trajectories of the bounding pair in the position space. This assertion follows directly from the preceding argument, and will become more clear when we come to the terminal path angles under the next heading. Mathematically, we may express this fact by

$$r_{*L} \leqslant r_{**} \leqslant r_{*H} \qquad (0 \leqslant \Delta\theta \leqslant \psi) \qquad (19)$$

where the three radial distances r_{*L}, r_{*H}, and r_{**} are taken along the same radius vector between the two terminal position vectors $\vec{r}_1$ and $\vec{r}_2$ as shown in Figure 8(a) (where equality signs in the foregoing formula hold only on the terminal radius vectors ($\Delta\theta = 0$, ψ). However, if they do hold on some intermediate radius vector, they will hold on every such radius vector, and the three trajectories, T_{*L}, T_{*H}, and T_{**} will coincide, a case in which the minimal two-impulse solution and the two minimal one-impulse solutions are identical, as presented in Section V-E. This special case will be excluded in the following analysis.

B. The Terminal Quantities

Direction of Departure and Arrival

40

(a) TRANSFER PLANE

(b) HODOGRAPH PLANE
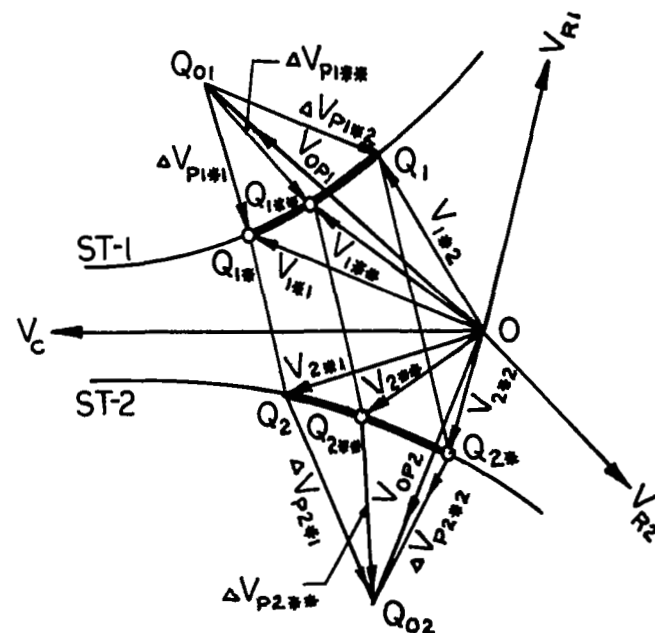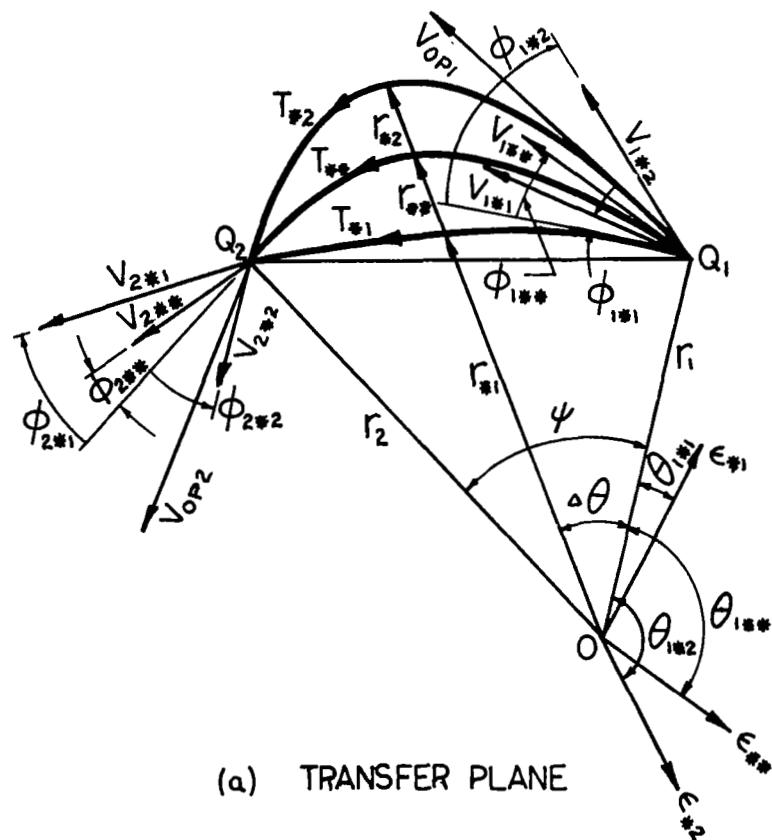
FIG. 8   THE MINIMAL TWO-IMPULSE TRANSFER TRAJECTORY AND ITS BOUNDING TRAJECTORIES.

Consider a typical optimal transfer arc pair as shown
in Figure 8(b), the geometry shows clearly that the three
path angles ϕ_{*L}, ϕ_{*H}, and ϕ_{**} at the initial point satisfy
the inequality

$$\phi_{1*L} < \phi_{1**} < \phi_{1*H} \qquad (20\text{-}1)$$

which is, in fact, the basis for the Inequality (19)
Thus, the high trajectory of a bounding pair has also a high
initial path angle, and vice versa. However, at the final
terminal point the roles of the high and low trajectories
are reversed, and we have

$$\phi_{2*H} < \phi_{2**} < \phi_{2*L} \qquad (20\text{-}2)$$

which is also evident from Figure 8(b). It is to be noted
that, although the reference here is made to Figure 8(b), in
which a transfer arc pair of short kind is shown, Inequalities
(20-1,2) hold equally well for the long kind of transfer, if
we always measure the path angle ϕ_i from the transversal
direction in the direction of motion, hence, limiting it to
$-\frac{\pi}{2} < \phi_i < \frac{\pi}{2}$ in each kind. These inequalities show that a
minimal two-impulse transfer trajectory is bounded by its
bounding trajectory pair in the directions of departure as
well as arrival.

The Transfer Velocities and Their Components

In view of Godal's compatibility condition, Equation (4), the chordal and radial components of the terminal transfer velocities change monotonically along the constraining hyperbola. Thus, with the aid of Figure 8(b), we deduce

$$V_{R*L} < V_{R**} < V_{R*H} \tag{21}$$

and

$$V_{C*H} < V_{C**} < V_{C*L} \tag{22}$$

From Inequality (22) we further deduce for the transversal component,

$$(V_{\theta i})_{*H} < (V_{\theta i})_{**} < (V_{\theta i})_{*L} \quad (i = 1,2) \tag{23}$$

since $V_{\theta i}$ is proportional to V_C. No such simple statement is available for the other component V_r of the coordinate pair (V_r, V_θ) as it is more involved. From Inequalities (21 to 23) we see that each of the three terminal transfer velocity components V_{R**}, V_{C**}, and $(V_{\theta i})_{**}$ is bounded between the corresponding components of the bounding trajectory pair. However, this is not always true for the resultant transfer velocities, as it will be seen below.

In dealing with the resultant velocity at either terminal, it is important to note that, for the transfer between two fixed terminal points, there exists an overall minimum velocity at each terminal, given by the minimum energy points, which is the vertex of the branch of the terminal constraining hyperbola (see Table C-2, Appendix C). Thus, it is essential

to distinguish whether the optimal transfer arc contains the minimum energy point or not. A study of the hodograph geometry enables one to deduce that, when the optimal arc contains no minimum energy point,

$$V_{i^*L} < V_{i^{**}} < V_{i^*H} \quad \text{if} \quad V_{i^*L} < V_{i^*H}$$

$$\quad (i = 1.2) \quad (24)$$

$$V_{i^*H} < V_{i^{**}} < V_{i^*L} \quad \text{if} \quad V_{i^*L} > V_{*H}$$

In case it does contain such a point, we replace the lower bound by $(V_i)_{min.}$ which has the magnitude,

$$(V_i)_{min.} = A_i = \sqrt{\frac{2\mu}{r_i} \tan \frac{\psi}{2} \tan \frac{\varphi_i}{2}} \quad (25)$$

The Terminal Velocity Impulses

With reference to Fig. 8(b), it is evident that

$$(\Delta V_{P1})_{*1} < (\Delta V_{P1})_{**} < (\Delta V_{P1})_{*2} \quad (26-1)$$

$$(\Delta V_{P2})_{*2} < (\Delta V_{P2})_{**} < (\Delta V_{P2})_{*1} \quad (26-2)$$

where the ΔV_P's are the in-plane velocity impulses. Going from these in-plane components to the resultants in the noncoplanar case, we note first that the out-of-plane terminal velocity components, (V_{ONi}) if present, do not alter the location of the minimal 2-impulse solution in the hodograph plane; and second, that under fixed terminal conditions, such a component is a constant at each terminal, hence, its effect on each velocity impulse at the same terminal is to increase it by a constant component in accordance with

$$f_i = \sqrt{(\Delta V_{Pi})^2 + V_{ONi}^2} \qquad (27)$$

Consequently, the preceding inequalities hold also for the resultant velocity impulses at each terminal:

$$f_{1*1} < f_{1**} < f_{1*2} \qquad (28\text{-}1)$$

$$f_{2*2} < f_{2**} < f_{2*1} \qquad (28\text{-}2)$$

from which we obtain immediately by addition,

$$f_{1*1} + f_{2*2} < f_{**} < f_{1*2} + f_{2*1} \qquad (29)$$

Thus, each of the two terminal velocity impulses and their sum required for a minimal 2-impulse transfer are well bounded, with their upper and lower bounds given by the two minimal 1-impulse solutions. In fact, two smaller upper bounds for f_{**} can be found to be

$$f_{*1} \equiv f_{1*1} + f_{2*1} \qquad (30\text{-}1)$$

$$f_{*2} \equiv f_{1*2} + f_{2*2} \qquad (30\text{-}2)$$

where f_{*1} is the sum of the two terminal impulses required on T_{*1}, and f_{*2}, that on T_{*2}, since

$$f_{**} < f_{*1} \qquad (31\text{-}1)$$

$$f_{**} < f_{*2} \qquad (31\text{-}2)$$

by definition. That the quantities f_{*1} and f_{*2} are both less than the upper bounds in the Inequality (29) can be easily seen since, again by definition, we have

$$f_{1*1} < f_{1*2} \quad , \quad f_{2*2} < f_{2*1} \qquad (32)$$

45

C. The Trajectory Elements

The Angular Momentum and the Semilatus Rectum

Noting that the angular momentum h is related to the chordal component V_C of a terminal transfer velocity by

$$h = V_C d \tag{33}$$

and that the distance d is a constant for the transfer between two fixed terminal points, we obtain immediately from Inequality (22),

$$h_{*H} < h_{**} < h_{*L} \tag{34}$$

which also implies that

$$\bar{r}_{*H} < \bar{r}_{**} < \bar{r}_{*L} \tag{35}$$

in view of the orbital relation,

$$\bar{r} = h^2/\mu \tag{36}$$

where $\bar{r}$ is the semilatus rectum of the trajectory conic.

The Orbital Energy and the Semimajor Axis

From the Vis Viva Integral,

$$k = \tfrac{1}{2}V^2 - \frac{\mu}{r} \tag{37}$$

we see that, to compare the orbital energies of different trajectories through the same terminal point, we need only to compare the magnitudes of their velocities. Here again the presence or absence of a minimum energy point in the optimal arc under consideration is of importance, and inequalities similar to those for the transfer velocities may be written

for the orbital energy as follows:

In the absence of the minimum energy point,

$$k_{*L} < k_{**} < k_{*H} \qquad \text{if} \qquad k_{*L} < k_{*H}$$

$$k_{*H} < k_{**} < k_{*L} \qquad \text{if} \qquad k_{*L} > k_{*H} \qquad (38)$$

In case such a point is present, we replace the lower bounds in the preceding inequalities by $k_{min.}$, which, in terms of the terminal parameters, is given by

$$k_{min.} = - \frac{2\mu}{r_1 + r_2 + \ell} \qquad (39)$$

The semimajor axis (a) of a trajectory conic in a given Newtonian field depends only on the orbital energy through the relation,

$$a = \frac{\mu}{2|k|} \qquad (40)$$

However, while k changes continuously along a constraining hyperbola, "a" changes discontinuously at the critical point Q^*; it also has a local minimum in the elliptic portion at the minimum energy point. Thus, to establish the upper and lower bounds for the semimajor axis of a minimal 2-impulse transfer trajectory, it is essential to examine whether the optimal arc contains a minimal energy point, or a critical point. When both points are absent, we have

$$a_{*L} < a_{**} < a_{*H} \qquad \text{if} \qquad a_{*L} < a_{*H}$$

$$a_{*H} < a_{**} < a_{*L} \qquad \text{if} \qquad a_{*L} > a_{*H} \qquad (41)$$

Whenever the optimal arc contains a critical point, we replace

47

the upper bounds in the preceding inequalities by ∞. When
it contains the minimum energy point alone, we replace the
lower bounds by the elliptic minimum a, given by [18]

$$a_{min.} = \tfrac{1}{4}(r_1 + r_2 + \ell) \tag{42}$$

However, when it contains both points, while we still replace
the upper bounds in the preceding inequalities by ∞, care
must be taken concerning the lower bound, since an hyperbolic
semimajor axis may be well smaller than the elliptic minimum.
Thus, in this case, we replace the lower bounds in Inequali-
ties (41) by a_{min} only when these bounds are greater
than a_{min}. The foregoing analysis shows that, while the
semimajor axis of T_{**} is bounded when T_{*1} and T_{*2} are both
elliptic, or both hyperbolic, or one of them is parabolic,
it is not necessary so when one of them is elliptic, and the
other is hyperbolic.

The Eccentricity Vector

Like the transfer velocity and orbital energy, there
exists in a 2-terminal trajectory family an overall minimum
for the numerical eccentricity, given by [18]

$$\epsilon_{min.} = \left| \frac{r_1 - r_2}{\ell} \right| \tag{43}$$

The point on the constraining hyperbola corresponding to this
least eccentric transfer trajectory is called the least
eccentricity point, and it can be shown that there is such a

point on each branch of a terminal constraining hyperbola, located as shown in Figure C-1. Thus, to establish the upper and lower bounds for the numerical eccentricity of the minimal 2-impulse transfer trajectory, it is essential to examine whether the optimal arc under consideration contains this least eccentricity point or not. Similar to the inequalities deduced for the terminal transfer velocity and the orbital energy, we have in the absence of the least eccentricity point,

$$\epsilon_{*L} < \epsilon_{**} < \epsilon_{*H} \quad \text{if} \quad \epsilon_{*L} < \epsilon_{*H}$$
$$\epsilon_{*H} < \epsilon_{**} < \epsilon_{*L} \quad \text{if} \quad \epsilon_{*L} > \epsilon_{*H} \tag{44}$$

In case the arc contains this least eccentricity point, we replace the lower bounds in the preceding inequalities by ϵ_{min}.

Furthermore, a study of the hodograph geometry shows that not only the numerical eccentricity of T_{**} is so bounded, but also the direction of its eccentricity vector which is in the direction of the apsidal axis. Denoting the angle between the eccentricity vector of a transfer trajectory and the terminal position vector $\vec{r}_i$ by θ_i, we have

$$\theta_{i*L} < \theta_{i**} < \theta_{i*H} \quad \text{if} \quad \theta_{i*L} < \theta_{i*H}$$
$$\theta_{i*H} < \theta_{i**} < \theta_{i*L} \quad \text{if} \quad \theta_{i*L} > \theta_{i*H} \qquad (i = 1.2) \tag{45}$$

Here the θ's are the true anomalies of the terminal point Q_i measured on the three trajectories, T_{*L}, T_{*H}, and T_{**} (see Fig. 8). So far as the bounding directions of the eccentricity

vectors are concerned, no reference to the least eccentricity point is necessary.

D. Time of Flight

It can be shown that the time of flight for the transfer between two fixed terminal points is a single-valued increasing function of the initial path angle. Thus, directly from Inequality (20-1) we deduce that

$$\Delta t_{*L} < \Delta t_{**} < \Delta t_{*H} \tag{46}$$

In addition to the few items presented above, the upper and lower bounds of many other trajectory quantities may be deduced in a similar way. However, no such exhaustive analysis will be attempted here. As a final remark, the following situation is worth mentioning:

When the two quantities, say X_{*1} and X_{*2} pertaining to a bounding trajectory pair, T_{*1} and T_{*2}, respectively, bound the corresponding quantity X_{**} of the minimal 2-impulse trajectory T_{**}, then the condition $X_{*1} = X_{*2}$ implies that

$$X_{**} = X_{*1} = X_{*2}$$

and

$$T_{**} = T_{*1} = T_{*2}$$

a case in which the minimal 2-impulse solution and the two minimal 1-impulse solutions are identical. However, this is not necessarily true when an absolute bound X_{abs}, upper or lower, is present unless $X_{*1} = X_{*2} = X_{abs}$.

For example, it is quite possible that a pair of bounding trajectories of the same eccentricity bounds a T_{**} of less eccentricity if the optimal arc contains the least eccentricity point. When this is the case, we observe that the two quantities X_{*1} and X_{*2}, being equal but distinct from X_{abs}, form an upper bound if X_{abs} is an absolute lower bound, and, a lower bound if X_{abs} is an absolute upper bound, and that they form no bound in the presence of both absolute upper and lower bounds.

VII. The Case of 180° Transfer

So far the analysis has been based on the assumption of $0 < \psi < \pi$. In the limiting case of $\psi = \pi$, although the stationarity Eqs. (6) and (13) no longer apply, the geometric analyses in Sections III and IV are still valid, and all the preceding qualitative and quantitative predictions still hold.

In fact, the situation is much simpler than in the general case, as the velocity constraining hyperbola for each terminal now degenerates into two straight lines both parallel to the line of terminals $Q_1 Q_2$, its evolute disappears, leaving the hodograph plane consisting of only the simple region, and the transfer arc pair now becomes a pair of two straight line segments. As consequences of such simpler hodograph geometry, and in line with the preceding general conclusions, the two-impulse 180° transfer presents some particular features as follows:

1. There is one and only one optimal transfer arc pair, hence, one and only one bounding trajectory pair, in each sense of transfer (the distinction between short and long transfers now ceases to exist).

2. No multi-minimum for the transfer in the same sense is possible; and there exists at most a double minimum of opposite senses (direct consequence of item 1).

3. The optimal condition for minimal two-impulse transfer, Eq. (5), reduces to

$$\sin \gamma_1 = \sin \gamma_2 \qquad (47)$$

for the 180° case. Here γ_i (i = 1,2) is the path angle of the velocity-increment vector $\Delta\vec{v}_i$ with reference to the local radial direction; hence, Eq. (47) expresses the Law of Equal Slope.

4. The coincidence condition reduces to simple

$$\vec{v}_{0r1} = \vec{v}_{0r2} \qquad (48)$$

5. In contrast with the non-180° transfer, the two position vectors, $\vec{r}_1$ and $\vec{r}_2$, now being collinear, do not determine the orientation of the transfer plane. Hence this orientation is open to choice.

Finally, it should be noted that, whereas no analytic solution in closed form is possible for the minimal two-impulse transfer in the general case, such a solution does exist in the 180° case. For such a solution and the further minimization of the total velocity impulse by optimizing the orientation of the transfer plane, the reader may consult Reference 27.
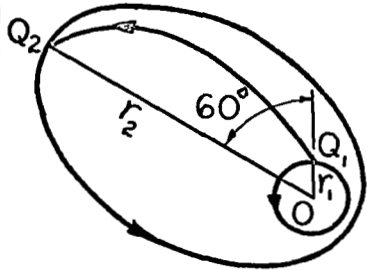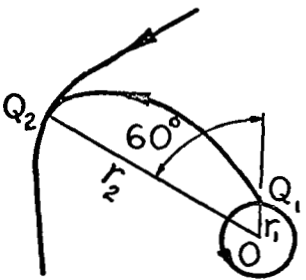
VIII. Numerical Examples

To verify the preceding predictions two sets of numerical examples have been worked out. The terminal conditions assumed and the corresponding transfer geometry are shown in Table 1. Set A consists of the transfers from a circular orbit to a series of coplanar, coaxial, and similar elliptic orbits of the same eccentricity 3/4 but varying size. The point of departure on the circular orbit is, in each case, at 60° from the point of arrival, which is the apocenter of the target ellipse. Both the initial and final orbits are assumed to be in the same sense of motion. Examples of set B are the same as those of set A, except that the final orbits are a series of similar hyperbolas of the same eccentricity 5/4, and that the point of arrival is the pericenter of the target hyperbola in each case. In each set of examples, the absolute minimal 2-impulse solution for T_{**}, and the two minimal 1-impulse solutions defining the bounding trajectory pair, T_{*1} and T_{*2}, are calculated for fixed values of the distance ratio n, ranging from 0.20 to 2.0. The principal results are graphically depicted in the nondimensional form in Figs. 9 to 14. Tabulated values are found in Appendix G, and some numerical results of particular interest are summarized in Table 1.

From these results, it is seen that each of the three principal trajectory parameters, V_C, V_R and h, calculated for

TABLE 1. NUMERICAL EXAMPLES OF THE MINIMAL TWO-IMPULSE ORBITAL TRANSFER

	(A) CIRCLE-TO-ELLIPSE		(B) CIRCLE-TO-HYPERBOLA	
TRANSFER GEOMETRY				
TERMINAL CONDITIONS	INITIAL	FINAL	INITIAL	FINAL
Orbital Eccentricities	$\varepsilon_1 = 0$	$\varepsilon_2 = 0.75$	$\varepsilon_1 = 0$	$\varepsilon_2 = 1.25$
Velocities	$\nu_{01} = 1$	$\nu_{02} = 0.5$	$\nu_{01} = 1$	$\nu_{02} = 1.5$
	$\phi_{01} = 0$	$\phi_{02} = 0$	$\phi_{01} = 0$	$\phi_{02} = 0$
Radial Distances	r_1	$r_2 = nr_1$	r_1	$r_2 = nr_1$
Angle of Separation	$\psi = 60°$		$\psi = 60°$	
Minimal Total Impulse, $f_{**}\big/\sqrt{\frac{\mu}{r_1}}$: lowest value	$= 0.5$ @ $n = 1.0$		$= 0.5$ @ $n = 1.0$	
Distance Ratio for $T_{**} = T_{*1} = T_{*2}$	$n_c = 0.630$		$n_c = 1.31$	

For detailed tabulated values, see Appendix G; for graphs, see Figs. 9 to 14.

T_{**} is indeed bounded between the corresponding quantities

for the two bounding trajectories, T_{*1} and T_{*2}, as predicted

by the Inequalities (21, 22, and 34). (See Figs. 9 to 11).

Also, the minimal total velocity impulse required

for the transfer is bounded between its upper and lower

bounds as predicted by Inequality (29)   (See Fig. 12).

To compare the total velocity impulses required for the

transfers along the three trajectories, T_{*1}, T_{*2}, and T_{**}, the

values of f_{*1}, f_{*2}, and f_{**} are found as shown in Fig. 13;

and the relative saving in the total velocity impulse by

2-impulse minimization over the minimization of each terminal

impulse is calcualted from

$$\frac{\Delta f_{*1}}{f_{*1}} = \frac{f_{*1} - f_{**}}{f_{*1}} \qquad (49-1)$$

$$\frac{\Delta f_{*2}}{f_{*2}} = \frac{f_{*2} - f_{**}}{f_{*2}} \qquad (49-2)$$

and graphically shown in Fig. 14.   From these plottings

it is seen that the f_{**} graph indeed remains below those of

f_{*1} and f_{*2}, as predicted by Inequalities (31-1,2), and that

the savings Δf_{*1} and Δf_{*2} are positive throughout, justifying

the two-impulse minimization.

In addition to the foregoing preliminary observations,

the following are worth noting:

1. For each of the trajectory parameters, V_C, V_R, and h,

calculated here, the three curves for the trajectories T_{**},

T_{*1} and T_{*2}, intersect at a common point, indicating the

coincidence of T_{*1}, T_{*2} and T_{**}. The same situations are found in the graphs of f_{**} and its upper and lower bounds as shown in Figs. 12, where the three curves f_{**}, f_{*1} and f_{*2} touch each other at their common point. The values of n at the common points given by the various graphs of the same set are, of course, the same. They are designated as n_c, as shown in Table 1. These values check with Eq. (18), as they should, since they belong to the class of apside-to-apside transfers.

2. For the inner transfer (n < 1) from a fixed initial terminal point, under constant angle of separation, and constant terminal velocities vectors, the total velocity impulse required for the transfer along each of the three trajectories, decreases as the final terminal distance r_2 increases; while in the outer transfer (n > 1), each of these impulses tend to increase with the final terminal distance within the present range of computation (see Figs. 12 and 13).

3. The case n = 1 is singular in each set of examples, since the initial circular orbit now passes through the final terminal point. Figures 9 to 11, and 13 show that each T_{**} - curve touches the T_{*1} curve at n = 1, indicating $T_{**}=T_{*1}\neq T_{*2}$. It is to be noted that, in examples B, the case of n = 0.722 is also singular since the final hyperbolic orbit now passes through the initial terminal point, and itself is T_{*2}. This is confirmed by the present computation as the value of f_{2*2} is indeed zero at this particular value of n. However, the computation results indicate that the absolute minimal T_{**} is

different from T_{*2} in this case. It can be verified that $\dot{n}=2.5$ is another singular case in example A, though beyond the present range of plotting, since the final elliptic orbit now passes through the initial terminal point.
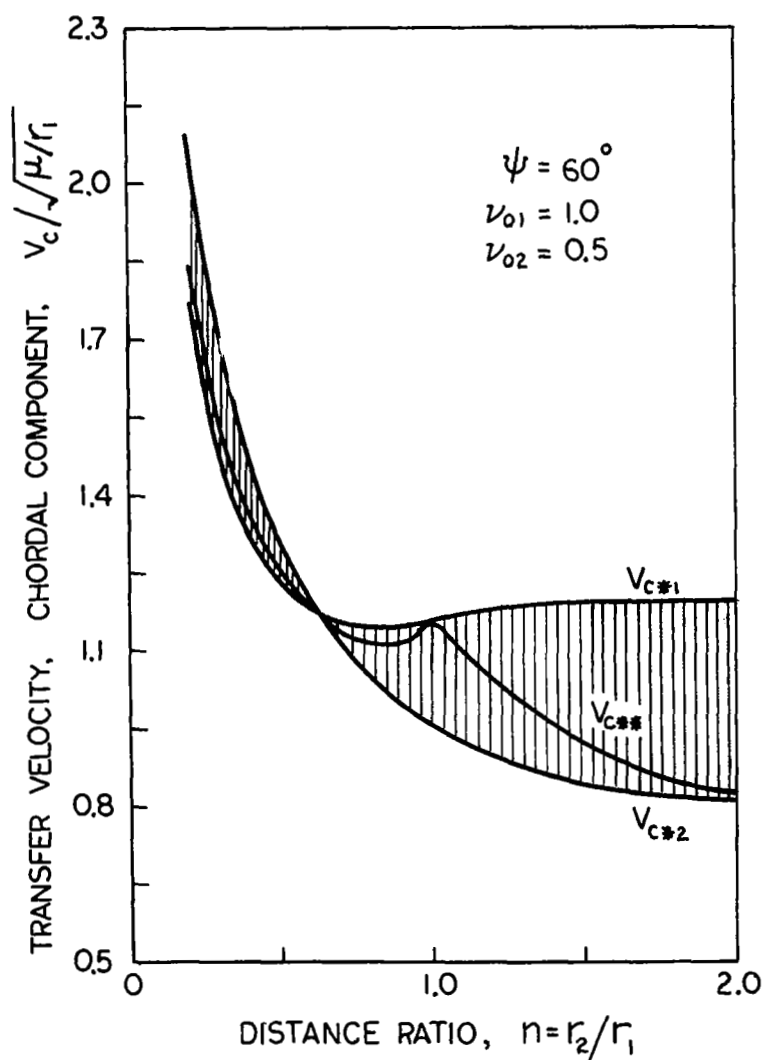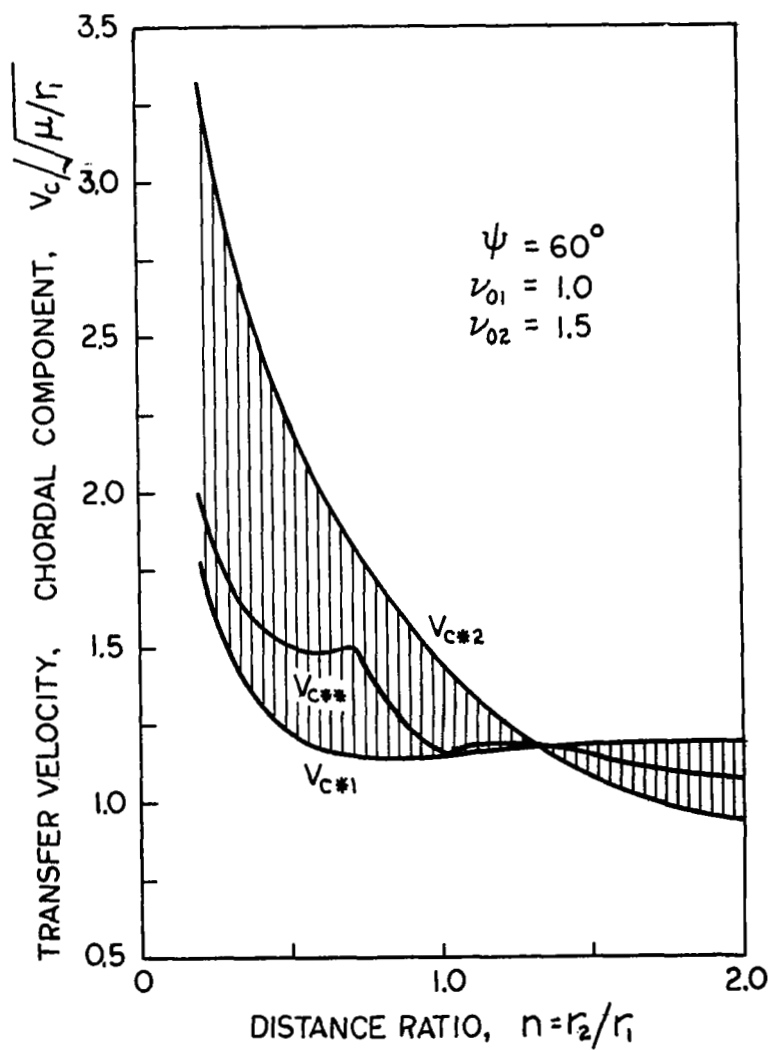
Fig 9   THE CHORDAL COMPONENT OF THE TERMINAL VELOCITY FOR MINIMAL
2-IMPULSE TRANSFER AND ITS UPPER AND LOWER BOUNDS
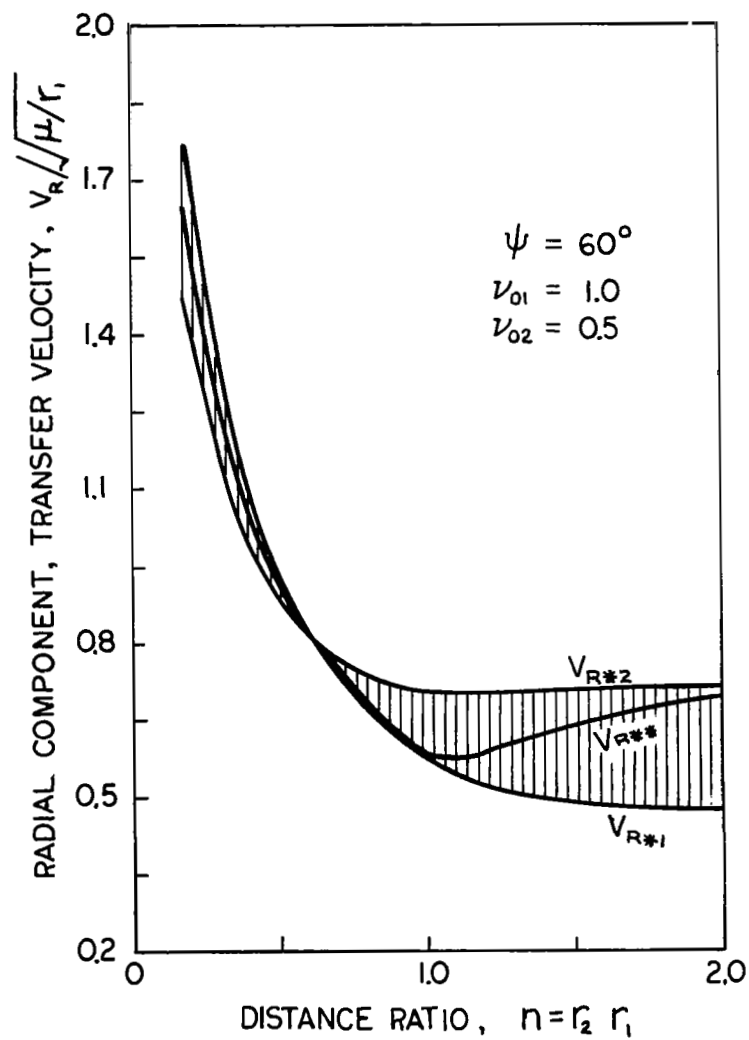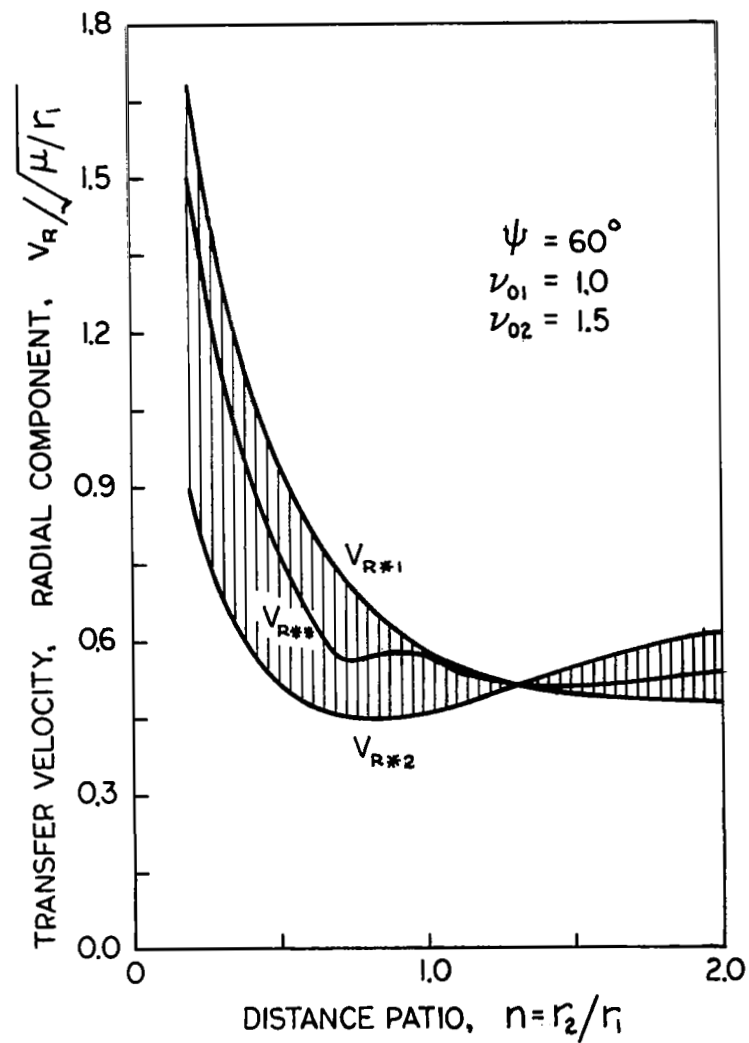
Fig. 10 THE RADIAL COMPONENT OF THE TERMINAL VELOCITY FOR MINIMAL
2-IMPULSE TRANSFER AND ITS UPPER AND LOWER BOUNDS
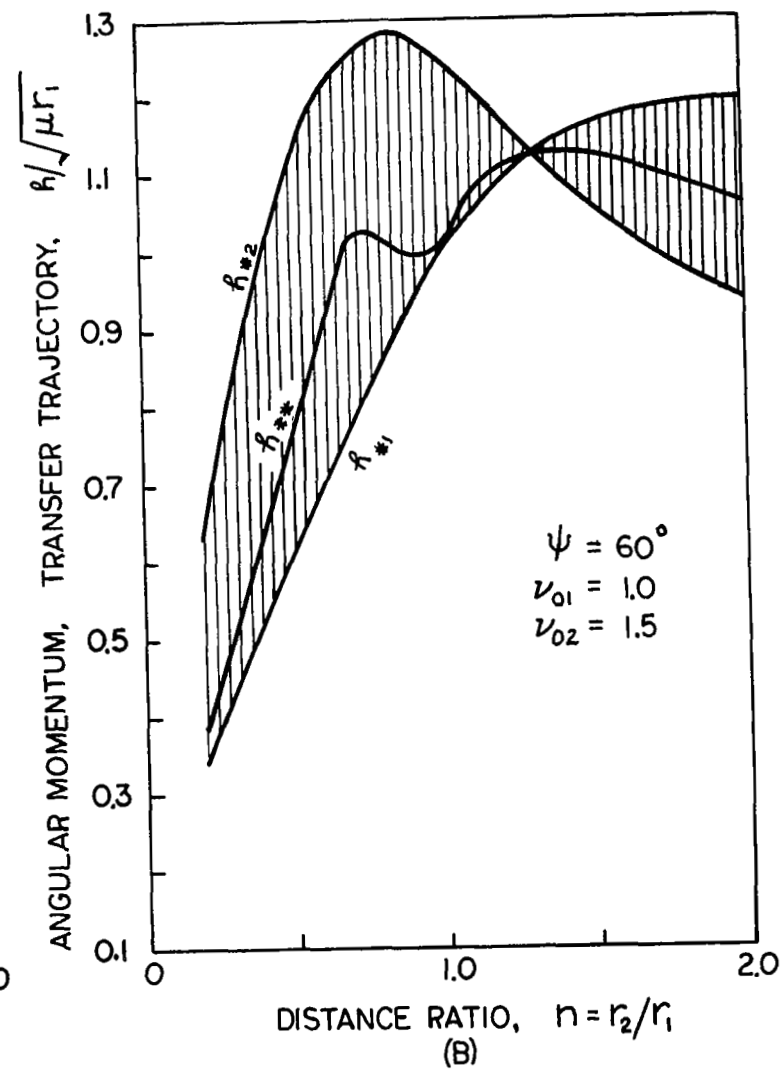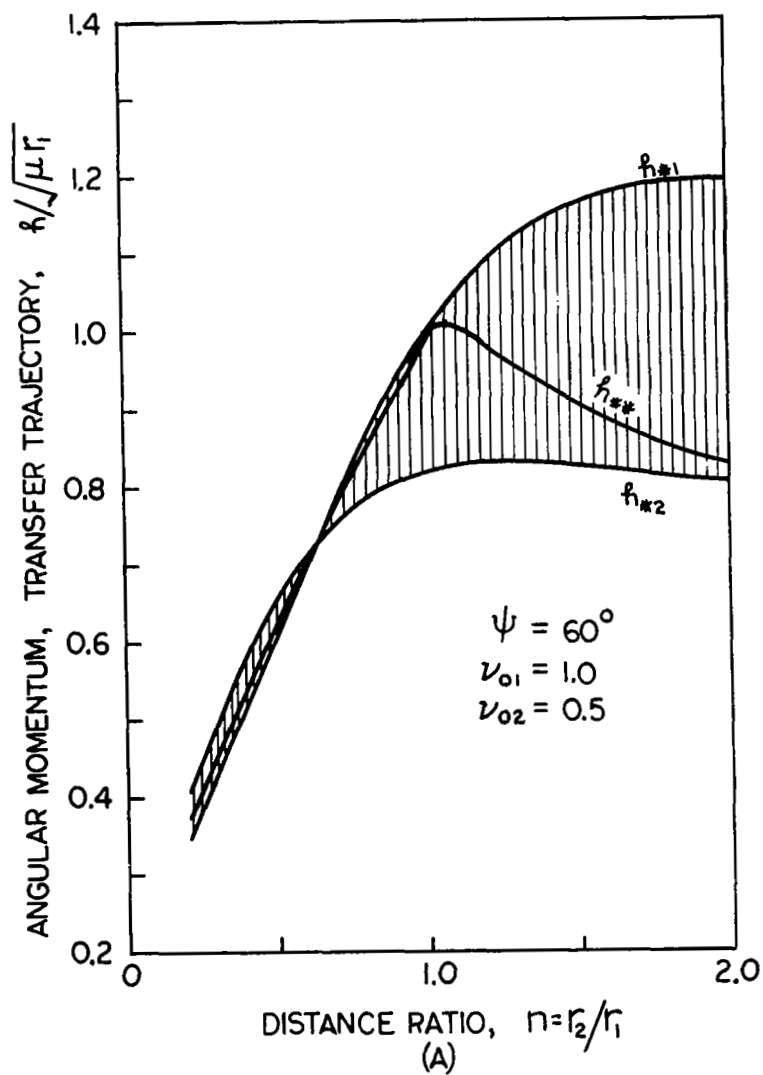
FIG. 11 THE ANGULAR MOMENTUM FOR MINIMAL 2-IMPULSE TRANSFER AND ITS
UPPER AND LOWER BOUNDS
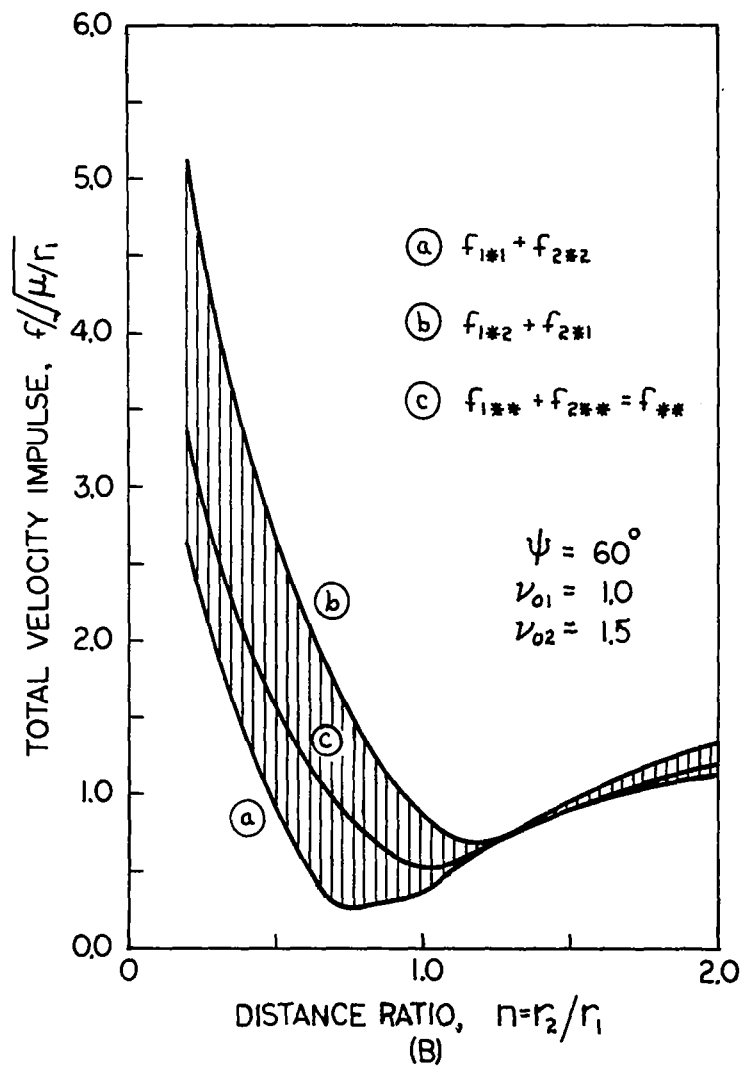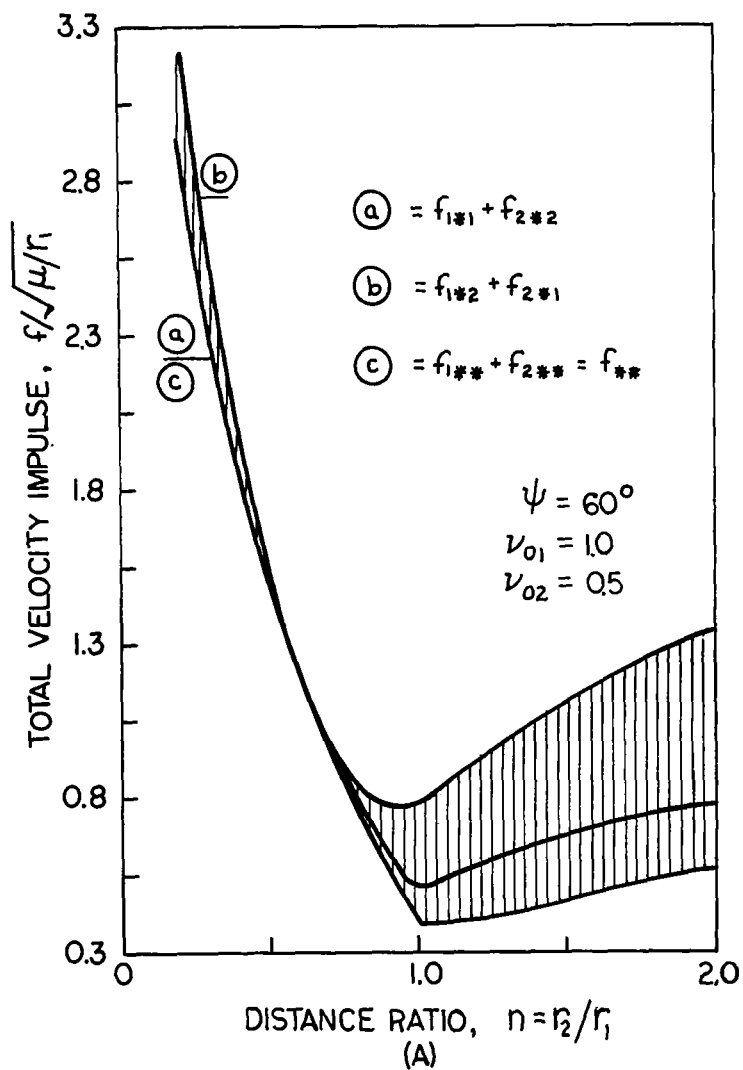
FIG. 12   THE MINIMAL TOTAL VELOCITY IMPULSE FOR 2-IMPULSE TRANSFER
AND ITS UPPER AND LOWER BOUNDS.
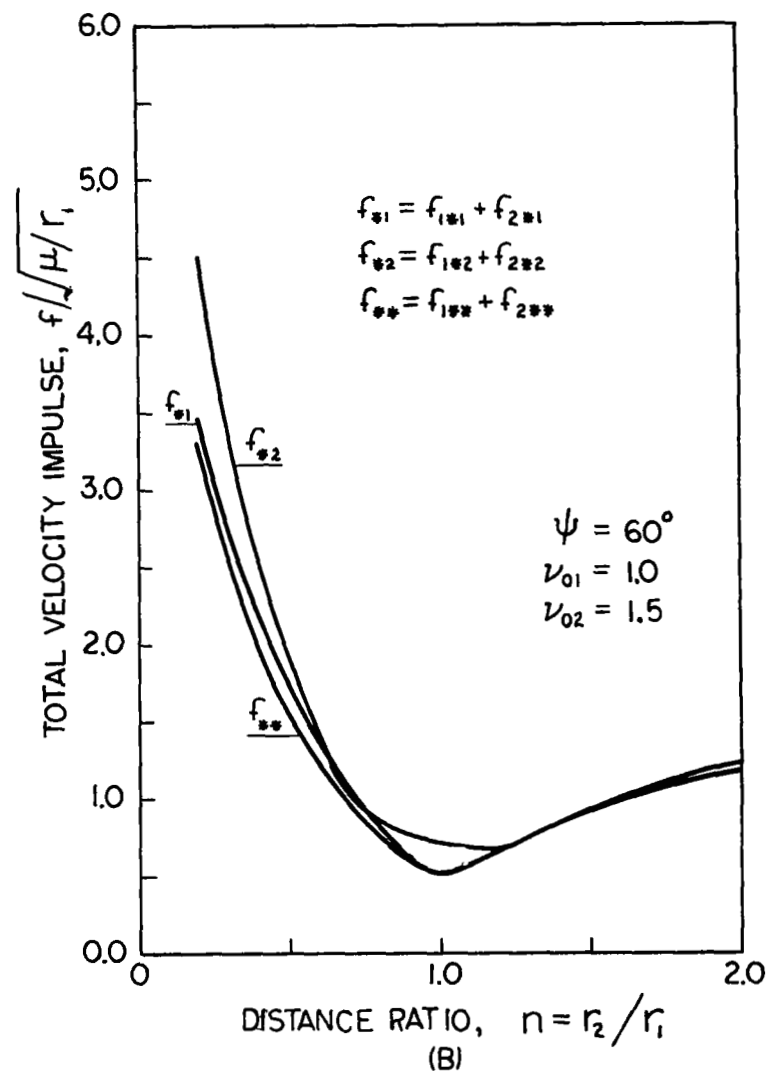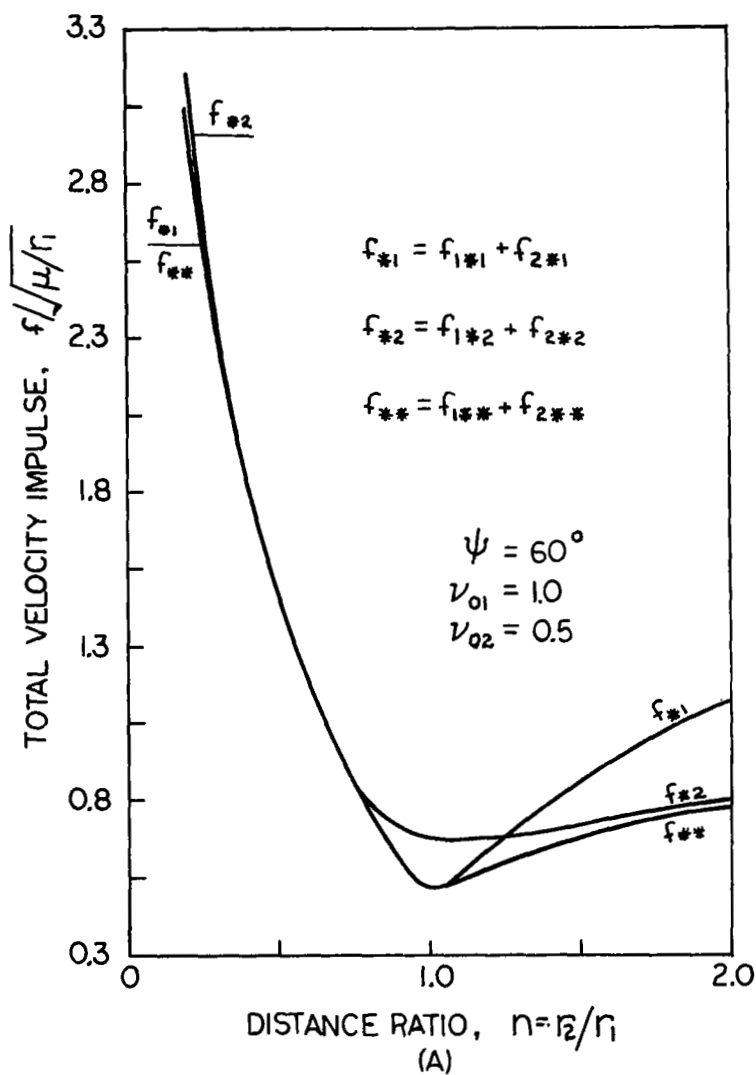
FIG. 13 THE TOTAL VELOCITY IMPULSES; THE MINIMAL 2-IMPULSE SOLUTION VERSUS THE MINIMAL INITIAL IMPULSE AND MINIMAL FINAL IMPULSE SOLUTIONS
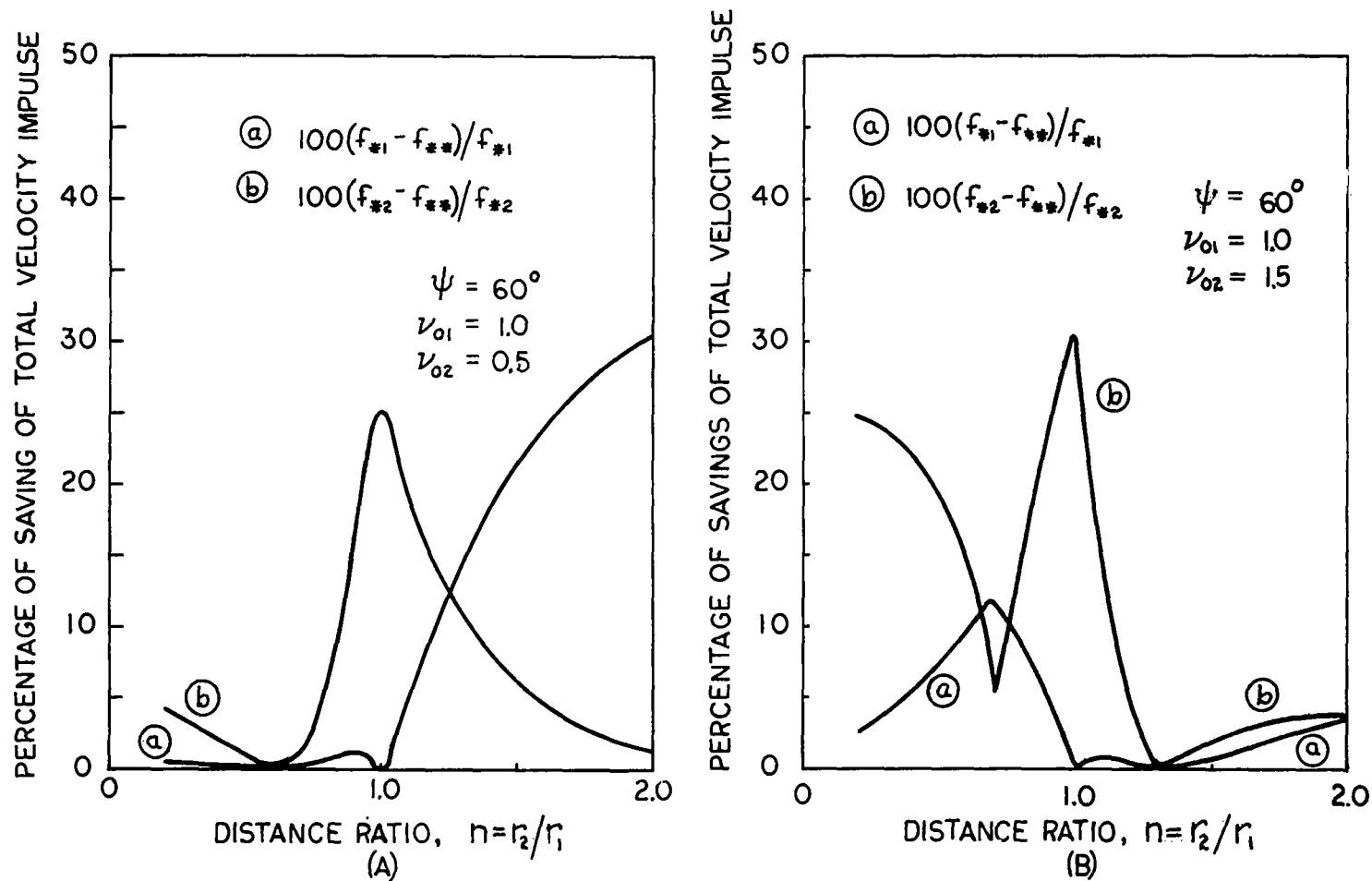
FIG. 14 PERCENTAGE OF SAVING IN TOTAL VELOCITY IMPULSES, 2-IMPULSE
MINIMIZATION OVER THE INITIAL IMPULSE MINIMIZATION AND
FINAL IMPULSE MINIMIZATION

IX.   Summary of Conclusions

1.   A minimal 2-impulse transfer trajectory T_{**} is bounded between a pair of bounding trajectories between the same terminal points in the same sense of motion, one T_{*_1} with a minimal initial impulse, and the other (T_{*_2}), a minimal final impulse.

It is not only bounded by the two bounding trajectories, in the position space, but also in spaces of other trajectory parameters, such as (a) the directions of departure and arrival, (b) the terminal transfer velocities and their components, V_C, V_R and V_Θ, (c) the terminal velocity impulses, (d) the angular momentum and semilatus rectum, (e) the orbital energy and semimajor axis, (f) the eccentricity vector, (g) time of flight, etc.

Under each item the trajectory quantities, X_{*_1} and X_{*_2}, pertaining to the bounding trajectory pair, T_{*_1} and T_{*_2} respectively, form a pair of upper and lower bounds of the corresponding quantity X_{**} pertaining to the trajectory T_{**} if no absolute upper and lower bounds are present. In case there exists an absolute bound, upper or lower, then it furnishes an additional choice for the proper bound X_{*_1} and X_{*_2}. (For details, see Section VI.)

2.   A minimal 2-impulse transfer trajectory always agree with its bounding trajectory pair in kind (short or long transfer), sense (counterclockwise or clockwise), type (elliptic, parabolic, or hyperbolic), and nature (realistic

67

or unrealistic) if they agree themselves; but not necessarily so with the two terminal orbits.

3. Under any terminal conditions, there exists at least one pair of bounding trajectories of each kind and sense; hence at least a local minimal 2-impulse solution, realistic or unrealistic, of each kind and sense.

4. There exist at most three bounding trajectory pairs of the same kind and sense, and at most a total of four such pairs of both kinds and senses. Hence there can be no more than a triple minimum of the same kind and sense of transfer and no more than a quadruple minimum of both kinds and senses.

5. Whenever the two trajectories of a bounding pair are coincident, the minimal 2-impulse transfer trajectory bounded between will coincide with them. A definite relation exists among the four terminal vectors, $\vec{r}_1$, $\vec{r}_2$, $\vec{V}_{01}$, and $\vec{V}_{02}$, for such coincidence (see Eq. (15)). When and only when this coincidence condition is met, the 2-impulse minimization and the 1-impulse minimizations at the initial and final terminals separately will yield the same transfer trajectory.

All the foregoing conclusions are valid for any arbitrary central angle $0 < \Psi < \pi$. For the particular conclusions pertaining to the case of $\Psi = \pi$, see Section VII.

X. Final Remarks

As shown in the preceding Sections, a great deal of information concerning the minimal 2-impulse transfer may be obtained once the two bounding trajectories are determined. In many cases, definite qualitative conclusions may be asserted directly from the bounding trajectory pair; and quantitatively, the upper and lower bounds of the principal parameters pertaining to the minimal 2-impulse transfer may be established. Since each bounding trajectory is governed by a quartic equation, while the minimal 2-impulse transfer trajectory is governed by an octic equation, the present treatment amounts to solving two fourth degree equations instead of one eighth degree equation. In view of the fact that a quartic equation is much more tractable than an octic, and that an analytic solution in closed form exists for the former, such a treatment is advisable. The present geometric approach in the hodograph plane by examining the optimal transfer arc pairs, rather than an algebraic approach to the solutions of the pertinent equations, has the further advantage of eliminating the extraneous roots of the governing octic, which do not belong to the stationarity solution, as well as the roots for the maximal total impulse solutions, so that the problem narrows down to locating all the local minimal solutions and choosing an absolute minimal and realistic one. As each bounding trajectory has the particular

significance of having a stationarity impulse at one terminal, the existing knowledge on the comparatively simpler problem of determining the optimal 1-impulse transfer trajectory[8, 20] may be utilized to aid the solution of the 2-impulse problem. Thus, in summary, the advantage of using the bounding trajectories for treating the 2-impulse transfer problem are as follows:

1. Solution of two quartic equations instead of a single but cumbersome octic equation.

2. Utilization of the existing knowledge on the optimal 1-impulse transfer problem to aid the solution of the optimal 2-impulse transfer problem.

3. The choice of a proper bounding trajectory pair eliminates the extraneous solutions as well as the maximal total impulse solutions.

At first sight it seems that the choice of a bounding trajectory pair is generally not unique, since each stationary quartic may yield as many as four distinct stationary 1-impulse trajectories. However, the present study shows that the number of such trajectory pairs cannot exceed three in one kind of transfer, and the total number of such pairs, counting both kinds, cannot exceed four (see Section V-D). Thus the number of possible bounding trajectory pairs is highly limited. In fact, the presence of three bounding

trajectory pairs of the same kind can happen only under the
condition that both terminal velocities enter the nonsimple
regions in the hodograph plane. This condition requires
that each terminal velocity be of sufficient magnitude,
$V_{0pi} > S_i$ (see Fig. C-1 and Eq. C-8, Appendix C), and that in
a direction with limited deviation from the minimal energy
direction, $(|\Phi_i| < \frac{\psi_i}{2}$, see Fig. C-1). Such a requirement puts
rather stringent conditions on the terminal orbits. For
example, in a coplanar $60°$-transfer at $n = 2$, it requires an
initial terminal velocity $V_{01} > 1.52\ V_1^*$ and a final terminal
velocity of $V_{02} > 4.13\ V_2^*$. Such conditions can be met only
between two hyperbolic orbits of the eccentricities $\varepsilon_1 > 3.62$
and $\varepsilon_2 > 3.34$, a combination not likely to be encountered in
practical problems. Thus in the usual cases, such as the
transfer between two moderately eccentric Keplerian orbits,
the two terminal velocity vectors will remain in the simple
regions, and consequently, there is a unique bounding trajec-
tory pair in each kind. Even under some unusual terminal
conditions, when one or both of the terminal velocities do
enter the nonsimple regions, and there are more than two
bounding trajectory pairs, the first choice will usually be
the pair of two absolute minimal 1-impulse transfer trajectories
if such a pair exists. Thus the proper choice of a bounding
trajectory pair, ordinarily does not present a problem.

In addition to yielding essential information on the

minimal 2-impulse transfer, the use of bounding trajectories

may also aid theoretical studies of such transfers. The

derivation of the coincidence condition, geometric as well

as analytic, for the identical 2-impulse minimization and

the two 1-impulse minimizations at the initial and final

terminals separately furnishes an example (see Section V-E).

Many other aspects of 2-terminal transfers may be investi-

gated in the light of the bounding trajectories; however,

such investigations are not intended in this report.

So far the present treatment has been kept perfectly

general without any restrictions on the terminal conditions

except that the two terminal orbits are assumed Keplerian.

Thus the predictions made are applicable to all particular

cases. In the case of 180° transfer, such predictions may

not be necessary, since an analytic solution exists[27], and

the computation is direct and simple. However, the application

of the bounding trajectory pair may still help to bring out

easily many salient features of such a transfer, as illustrated

in Section VII. No attempt is made here to cover other

particular cases. However, the application of the present

treatment to various cases under specialized terminal conditions

should be straight forward.

Finally, it should be mentioned that, when the number

of impulses are open to choice, three or more impulses may

prove to be more economical than two impulses under the same

initial and final terminal conditions in certain cases.[7,22,24,26]

Nevertheless, the two-impulse optimum will continue to be a

practical mode of optimal transfer in most cases even though

optimal solutions with additional impulse or impulses do exist as the penalties on the implementational complexity and the duration of transfer may well offset the additional saving in fuel economy. A full discussion of the general multi-impulse transfer problem, however, is beyond the scope of the present report.

REFERENCES

1. Hohmann, W., Die Erreichbarkeit der Himmelskorper, R. Oldenburg, Munich, 1925.

2. Lawden, D. F., The Determination of Minimal Orbits, J. British Interplanetary Soc., Vol. 11, 1952, pp. 216-224.

3. Vargo, L. G., Optimal Transfer Between Coplanar Terminals in a Gravitational Field, Advances in Astronautical Sciences, Vol. 3, Plenum Press, N.Y., 1958, pp. 20-1 to 20-9.

4. Th. Godal, Conditions of Compatibility of Terminal Positions and Velocities, Proceedings, XIth International Astronautical Congress, Stockholm, 1960.

5. Munick, H., McGill, R. and Taylor, G. E., Minimization of Characteristic Velocity for Two-Impulse Orbital Transfer, ARS J., Vol. 30, No. 7, July, 1960, pp. 638-639.

6. Lu Ting, Optimum Orbital Transfer by Impulses, ARS J., Vol. 30, No. 11, November, 1960, pp. 1013-1018.

7. Hoekler, R. F., and Silber, R., The Bi-Elliptical Transfer Between Coplanar Circular Orbits, Proceedings of the 4th AFBMD/STL Symposium 1959, Vol. III., Pergamon Press, 1961, pp. 164-175.

8. Stark, H. M., Optimum Trajectories Between Two Terminals in Space, ARS J., Vol. 31, No. 2, February, 1961, pp.261-263.

9. Rider, L., Characteristic Velocity Requirements for Impulsive Thrust Transfers Between Noncoplanar Circular Orbits, ARS J., Vol. 31, No. 3, March, 1961, pp. 345-351.

10. Lawden, D. F., Optimal Two-Impulse Transfer, Optimization Techniques, edited by G. Leitmenn, Academic Press, N.Y., 1962, pp. 333-348.

11. Horner, J. M., Optimum Impulsive Orbital Transfers Between Coplanar Orbits, ARS J., Vol. 32, No. 7, July, 1962, pp. 1082-1089.

12. Altman, S. P. and Pistiner, J., Minimum Velocity-Increment Solution for Two-Impulse Coplanar Orbital Transfer, AIAA J., Vol. 1, No. 2, February, 1963, pp. 435-442.

13. McCue, G. A., Optimum Two-Impulse Orbital Transfer and Rendezvous Between Inclined Elliptical Orbits, AIAA J. Vol. 1, No. 8, August, 1963, pp. 1865-1872.

14. Kirpichnikoc, S. N., Optimal Coplanar Flight Between Orbits, Vestnik Leningradeskogo Universiteta, No. 1, Leningrade, 1964, pp. 130-141 (English translation, NASA TT F-221, Washington, D.C.).

15. Breakwell, John V., Minimum Impulse Transfer, Progress in Astronautics and Aeronautics, Vol. 14, Academic Press, 1964, pp. 583-589.

16. Lee, Gentry, An Analysis of Two-Impulse Orbital Transfer AIAA J., Vol. 2, No. 10, October, 1964, pp. 1767-1773.

17. Altman, S. P., and Pistiner, J. S., Analysis of the Orbital Transfer Problem in Three-Dimensional Space, Progress in Astronautics and Aeronautics, Vol. 14, Academic Press, 1964, pp. 627-654.

18. Sun, F. T., Hodograph Analysis of Free-Flight Trajectories Between Two Arbitrary Terminal Points, NASA CR-153, Washington, D.C., January, 1965.

19. Koenke, E. J., Minimum Two-Impulse Transfer Between Coplanar Circular Orbits, AIAA Paper No. 66-11, 3rd Aerospace Science Meeting, N.Y., January, 1966.

20. Sun, F. T., On the Optimum Transfer Between Two Terminal Points with Minimum Initial Impulse Under an Arbitrary Initial Velocity Vector, NASA CR-662, Nov., 1966.

21. Gobetz, F. W., Washington, M., and Edelbaum, T. N., Minimum-Impulse Time-Free Transfer Between Elliptic Orbits, NASA CR-636, November, 1966.

22. Marchal, C., Marec, J. P., and Winn, C. B., Synthese des resultats analytiques sur les transferts optimaux entre orbits Kelperiennes, 18th IAF Congress, Belgrade, 1967 (NASA TT F-11, 590, 1968).

23. Edelbaum, T. N., Minimum Impulse Transfers in the Near Vicinity of a Circular Orbit, Journal of Astronautical Sciences, Vol. 14, No. 2, March-April, 1967, pp. 66-73.

24. Edelbaum, T. N., How Many Impulses? Astronautics and Aeronautics, Vol. 5, No. 11, Nov. 1967, pp. 64-69.

25. Sun, F. T., Analysis of the Optimum Two-Impulse Orbital Transfer Under Arbitrary Terminal Conditions, AIAA Journal Vol. 6, No. 11, Nov. 1968, pp. 2145-2153.

26. Gobetz, F. W., and Doll, J. R., A Survey of Impulsive Trajectories, AIAA Journal Vol. 7, No. 5, May 1969, pp. 801-834.

27. Sun, F. T., Analytic Solution of the Optimal Two-Impulse 180° Transfer Between Noncoplanar Orbits and the Optimal Orientation of the Transfer Plane, AIAA Journal Vol. 7, No. 10, October, 1969, pp. 1898-1904.

APPENDIX A

Derivation of the Stationarity Octic Equations in Symmetric
Velocity Coordinates

In terms of the symmetric coordinates (V_C, V_R), the
terminal velocity impulse required for the transfer is given
by

$$f_i^2 = V_C^2 + V_R^2 - 2N_{oi}V_C - 2M_{oi}V_R + P_{oi} \qquad (i=1,2) \qquad (A-1)$$

where M_{oi}, N_{oi}, and P_{oi} are defined by Equations (7 to 10).
Carrying out the differentiation of Equation (A-1) as
indicated in Equation (5), and noting from Equation (4) the
differential relation

$$\frac{dV_C}{V_C} + \frac{dV_R}{V_R} = 0 \qquad (A-2)$$

we obtain, after simplification, the stationarity equation
in the symmetric form

$$a_4 V_{C**}^4 + a_3 V_{C**}^3 + a_2 V_{C**}^2 + a_1 V_{C**} + a_o + a_{-1}V_{R**}$$

$$+ a_{-2}V_{R**}^2 + a_{-3}V_{R**}^3 + a_{-4}V_{R**}^4 = 0 \qquad (A-3)$$

where

$$a_4 = N_{o1}^2 - N_{o2}^2 - P_{o1} + P_{o2}$$

$$a_3 = 4K(M_{o1} - M_{o2}) + 2N_{o1}N_{o2}(N_{o2} - N_{o1})$$

$$+ 2(N_{o2}P_{o1} - N_{o1}P_{o2})$$

$$a_2 = 2K(N_{o2}M_{o2} - N_{o1}M_{o1} + 4N_{o1}M_{o2} - 4N_{o2}M_{o1}) + N_{o1}^2 P_{o2} - N_{o2}^2 P_{o1}$$

$$a_1 = 4K^2(N_{o2} - N_{o1}) + 4KN_{o1}N_{o2}(M_{o1} - M_{o2})$$

$$+ 2K(M_{o1}P_{o2} - M_{o2}P_{o1} + M_{o1}N_{o2}^2 - M_{o2}N_{o1}^2)$$

$$a_o = K^2(M_{o1}^2 - M_{o2}^2 + N_{o1}^2 - N_{o2}^2) + 2K^2(P_{o1} - P_{o2})$$

$$+ 2K(N_{o2}M_{o2}P_{o1} - N_{o1}M_{o1}P_{o2})$$

$$a_{-1} = 4K^2(M_{o2} - M_{o1}) + 4KM_{o1}M_{o2}(N_{o1} - N_{o2})$$

$$+ 2K(N_{o1}P_{o2} - N_{o2}P_{o1} + N_{o1}M_{o2}^2 - N_{o2}M_{o1}^2)$$

$$a_{-2} = 2K(M_{o2}N_{o2} - M_{o1}N_{o1} + 4M_{o1}N_{o2} - 4M_{o2}N_{o1})$$

$$+ M_{o1}^2 P_{o2} - M_{o2}^2 P_{o1}$$

$$a_{-3} = 4K(N_{o1} - N_{o2}) + 2M_{o1}M_{o2}(M_{o2} - M_{o1})$$

$$+ 2(M_{o2}P_{o1} - M_{o1}P_{o2})$$

$$a_{-4} = M_{o1}^2 - M_{o2}^2 - P_{o1} + P_{o2} \qquad \text{(A-4)}$$

Eliminating V_C and then V_R alternately from Equations (A-3) and (4) results in the octics in V_C and V_R respectively:

$$\sum_{n=0}^{8} C_n V_{C**}^n = 0 \qquad (6\text{-}c)$$

$$\sum_{n=0}^{8} R_n V_{R**}^n = 0 \qquad (6\text{-}R)$$

where

$$C_n = a_{n-4}, \qquad R_n = a_{4-n} \qquad n = 4 \text{ to } 8 \qquad (A\text{-}5)$$

$$C_n = K^{4-n} a_{n-4}, \qquad R_n = K^{4-n} a_{4-n} \qquad n = 0 \text{ to } 4$$

Note here the reciprocal relations among the coefficients:

$$a_m = a_{-m}^T \qquad (A\text{-}6)$$

$$C_n = K^{4-n} C_{8-n}^T = R_n^T \qquad (A\text{-}7)$$

$$R_n = K^{4-n} R_{8-n}^T = C_n^T \qquad (A\text{-}8)$$

where the transpose (T) indicates the interchange of M_{oi} and N_{oi}.

TABLE B: PRINCIPAL TRAJECTORY PARAMETERS OF
TWO-IMPULSE TRANSFER IN SYMMETRIC
VELOCITY COORDINATES

	Basic Formulas
Transfer Velocity	
Magnitude	$V_i = \sqrt{V_C^2 + V_R^2 - 2K \cos \psi_i}$ (B-1)
(r, θ) components	$V_{ri} = V_R - V_C \cos \psi_i$ (B-2)
	$V_{\theta i} = V_C \sin \psi_i$ (B-3)
Path Angle	$\phi_i = \tan^{-1} \left(\dfrac{V_R}{V_C} \csc \psi_i - \cot \psi_i \right)$ (B-4)
Velocity-Increment (Terminal Impulse)	
Magnitude	$f_i = \sqrt{V_C^2 + V_R^2 - 2N_{oi}V_C - 2M_{oi}V_R + V_{oi}^2 - 2K \cos \phi_i}$ (B-5)
Direction Cosines	$\cos \gamma_{ri} = (V_R - V_C \cos \psi_i - V_{ori}) / f_i$ (B-6)
	$\cos \gamma_{\theta i} = (V_C \sin \phi_i - V_{o\theta i}) / f_i$ (B-7)
	$\cos \gamma_{Ni} = -V_{oNi} \, f_i$ (B-8)
Total Velocity-Impulse	$f = \sum_{i=1}^{2} \sqrt{V_C^2 + V_R^2 - 2N_{oi}V_C - 2M_{oi}V_R + V_{oi}^2 - 2K \cos \phi_i}$ (B-9)
Angular Momentum	$h = V_C r_i \sin \psi_i$ (B-10)
Orbital Energy	$k = \tfrac{1}{2}(V_C^2 + V_R^2) - K \cos \psi_i - \dfrac{\mu}{r_i}$ (B-11)

Nondimensional Formulas

$$\nu_i = \sqrt{\nu_{ci}^2 + \nu_{Ri}^2 - 2\tan\frac{\psi}{2}\cot\varphi_i} \qquad (B-1')$$

$$\nu_{ri} = \nu_{Ri} - \nu_{ci}\cos\varphi_i \qquad (B-2')$$

$$\nu_{\theta i} = \nu_{ci}\sin\varphi_i \qquad (B-3')$$

$$\phi_i = \tan^{-1}\left(\frac{\nu_R}{\nu_c}\csc\varphi_i - \cot\varphi_i\right) \qquad (B-4')$$

$$\frac{f_i}{\sqrt{\mu/r_i}} = \sqrt{\nu_c^2 + \nu_R^2 - 2n_{oi}\nu_c - 2m_{oi}\nu_R + \nu_{oi}^2 - 2\tan\frac{\psi}{2}\cot\varphi_i} \qquad (B-5')$$

$$\cos\gamma_{ri} = \left(\nu_R - \nu_c\cos\varphi_i - \nu_{ori}\right) \Big/ \frac{f_i}{\sqrt{\mu/r_i}} \qquad (B-6')$$

$$\cos\gamma_{\theta i} = \left(\nu_c\sin\varphi_i - \nu_{o\theta i}\right) \Big/ \frac{f_i}{\mu/r_i} \qquad (B-7')$$

$$\cos\gamma_{Ni} = -\nu_{oNi}\Big/\frac{f_i}{\sqrt{\mu/r_i}} \qquad (B-8')$$

$$\frac{f}{\sqrt{\mu/r_1}} = \sqrt{\nu_{c1}^2 + \nu_{R1}^2 - 2n_{o1}\nu_{c1} - 2m_{o1}\nu_{R1} + \nu_{o1}^2 - 2\tan\frac{\psi}{2}\cot\varphi_1}$$
$$+ \sqrt{\nu_{c2}^2 + \nu_{R2}^2 - 2n_{o2}\nu_{c2} - 2m_{o2}\nu_{R2} + \nu_{o2}^2 - 2\tan\frac{\psi}{2}\cot\varphi_2}\Big) \Big/n \qquad (B-9')$$

$$\frac{h}{\sqrt{\mu r_i}} = \nu_{ci}\sin\varphi_i \qquad (B-10')$$

$$\frac{k_i}{\mu/r_i} = \tfrac{1}{2}\left(\nu_{ci}^2 + \nu_{Ri}^2\right) - \tan\frac{\psi}{2}\cot\varphi_i - 1 \qquad (B-11')$$

APPENDIX C

GEOMETRY OF THE TERMINAL VELOCITY CONSTRAINING HYPERBOLA AND THE PERTINENT FORMULAS

TABLE C-1

The Principal Geometric Elements of the Constraining Hyperbola

$$(i = 1,2)$$

The Constraining Hyperbola		
Eq. in Rectangular Coordinates	$\dfrac{V_{\zeta i}^2}{A_i^2} - \dfrac{V_{\chi i}^2}{B_i^2} = 1$	(C-1)
Semitransversal Axis	$A_i = \sqrt{\dfrac{2\mu}{r_i} \tan \dfrac{\psi}{2} \tan \dfrac{\varphi_i}{2}}$	(C-2)
Semiconjugate Axis	$B_i = \sqrt{\dfrac{2\mu}{r_i} \tan \dfrac{\psi}{2} \cot \dfrac{\varphi_i}{2}}$	(C-3)
Center-to-Focus Distance	$C_i = \sqrt{\dfrac{\mu}{d} \tan \dfrac{\psi}{2}}$	(C-4)
Eccentricity	$e_i = \csc \dfrac{\varphi_i}{2}$	(C-5)
Included Angle Between the Asymptotes	$\sigma_i = \pi - \varphi_i$	(C-6)
The Evolute - Lamé		
Eq. in Rectangular Coordinates	$(A_i V_{\zeta i})^{\frac{2}{3}} - (B_i V_{\chi i})^{\frac{2}{3}} = C^{\frac{4}{3}}$	(C-7)
Center-to-Vertex Distance	$S_i = \sqrt{\dfrac{2\mu}{r_i} \tan \dfrac{\psi}{2} \tan \dfrac{\varphi_i}{2}} \Big/ \sin^2 \dfrac{\varphi_i}{2}$	(C-8)
Included Angle Between the Asymptotes	$\sigma_i = \varphi_i$	(C-9)

Notes:

1. The constraining hyperbola is asymptotic to the
terminal radial direction and the chordal direction, while
its involute, a form of Lame', is asymptotic to the terminal
transversal direction and the direction perpendicular to
the chord. The two sets of asymptotic directions are thus
orthogonal to each other.

2. The constraining hyperbola and its involute have the
interior and exterial bisectors of the base angle at the
terminal as their common transversal and common conjugate axes
respectively.

(A typical terminal constraining hyperbola is shown in Fig. C-1.
For the particular points of interest on the constraining hyperbola,
See Table C-2. For the relative orientation of the two terminal
constraining hyperbolas, see Fig. 4.)
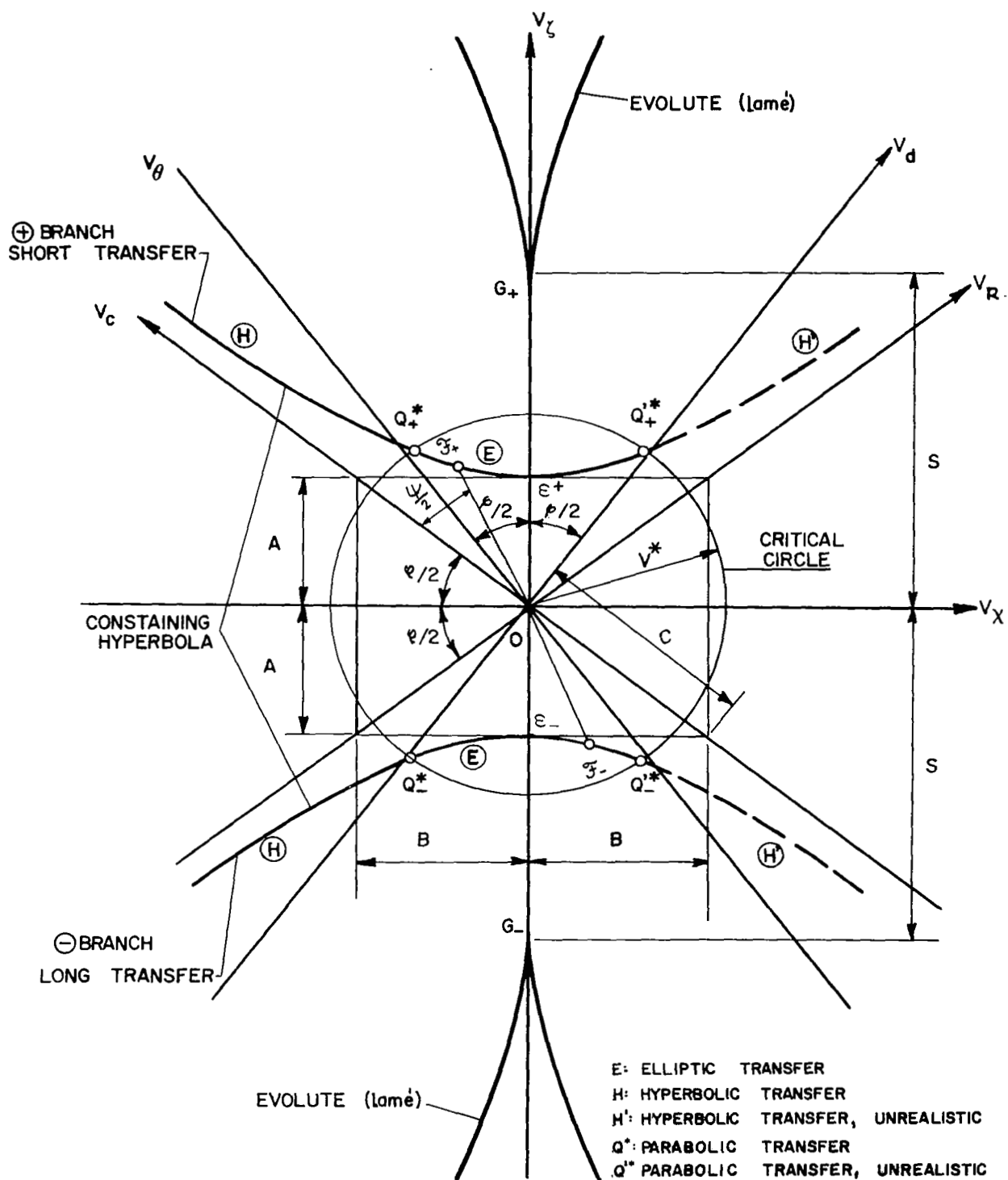
FIG. C-I   THE TERMINAL VELOCITY CONSTRAINING HYPERBOLA AND ITS EVOLUTE

TABLE C-2:   PARTICULAR POINTS ON THE TERMINAL CONSTRAINING
HYPERBOLA AND THEIR ASSOCIATED TRAJECTORIES

Transfer Trajectory	Points on the Constraining Hyperbola			Pertinent Formulas (i = 1.2)	
	Designation		Location		
	ST	LT			
Minimum Energy	$\mathcal{E}_+$	$\mathcal{E}_-$	Vertex of each branch	$(V_i)_{min.} = A_i$	(C-10)
				$k_{min.} = -\dfrac{2\mu}{r_1 + r_2 + \ell}$	(C-11)
				$a_{min.} = \tfrac{1}{4}(r_1 + r_2 + \ell)$	(C-12)
Least Eccentricity	$\mathcal{F}_+$	$\mathcal{F}_-$	See Fig. C-1	$\min. = \dfrac{\left| r_1 - r_2 \right|}{\ell}$	(C-13)
Critical (Parabolic)			Intersections of the critical circle with the constraining hyperbola		
Realistic	Q_+^*	Q_-^*		$v_i^* = \sqrt{\dfrac{2\mu}{r_i}}$	(C-14)
Unrealistic	Q_+^{1*}	Q_-^{1*}		$\tan \Phi_1^* = \sqrt{\cot \dfrac{\varphi_1}{2} \tan \dfrac{\varphi_2}{2}}$	(C-15-1)
				$\tan \Phi_2^* = \sqrt{\tan \dfrac{\varphi_1}{2} \cot \dfrac{\varphi_2}{2}}$	(C-15-2)

TABLE D: TERMINAL CONDITIONS AND THE DISTRIBUTION OF ORTHOPOINTS AND THEIR ASSOCIATED STATIONARY ONE-IMPULSE TRANSFER TRAJECTORIES†

Location of Terminal Velocity Point Q_{oi}	Location of Orthopoints and Types of the Associated Transfer Trajectories			
	Q_{i*a}	Q_{i*b}	Q_{i*c}	Q_{i*d}
EE - S ±	E ±	----	----	E ∓
EE - N ±	E ±	E ±	E ±	E ∓
HE - S ±	H ±	----	----	E ∓
HE - N ±	H ±	H'± (E∓)	H'± (E∓)	E ∓
HH - S ±	H ±	----	----	H ∓
Boundary between EE & HE: S ±	Q*±	----	----	E ∓
N ±	Q*±	E ±	E ±	E ∓
Boundary between HE & HH: S ±	H ±	----	----	Q*∓
H'E - S±	H'±	----	----	E ∓
H'E - N±	H'±	H ± (E∓)	H ±(E±)	E ∓
H'H' - S±	H'±	----	----	H'∓

Notations: ' unrealistic transfer, + short transfer, - long transfer; for others, see nomenclature.

---

† Symbols in parenthesis are for the hatched portion of the HE-N± or H'E-N± regions only, see Figs. 5 and D-1.
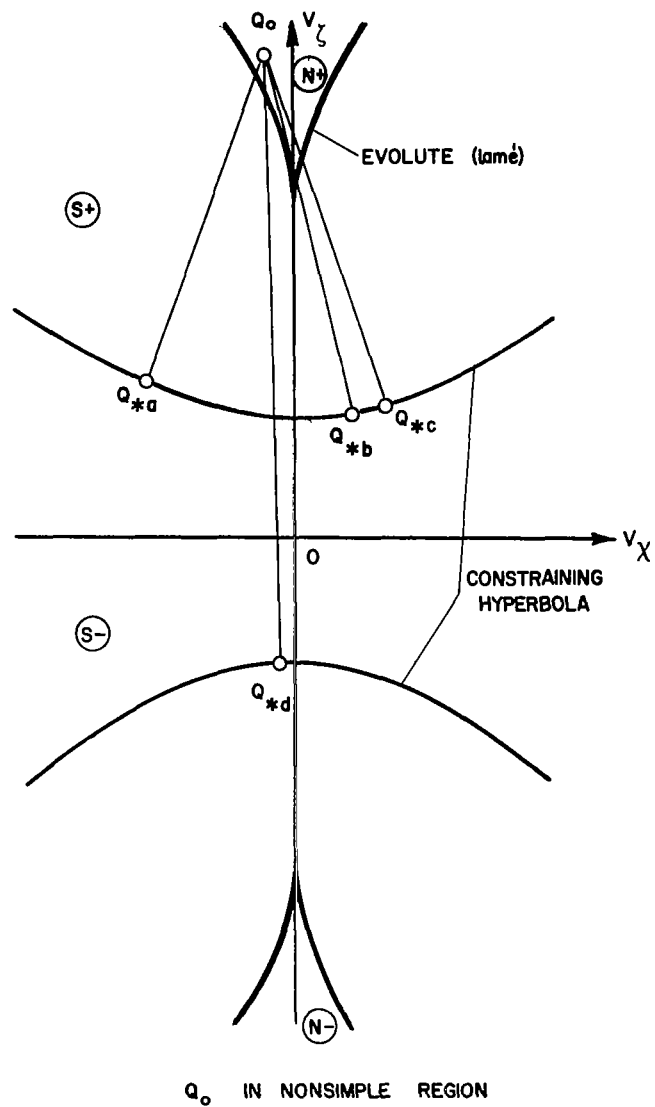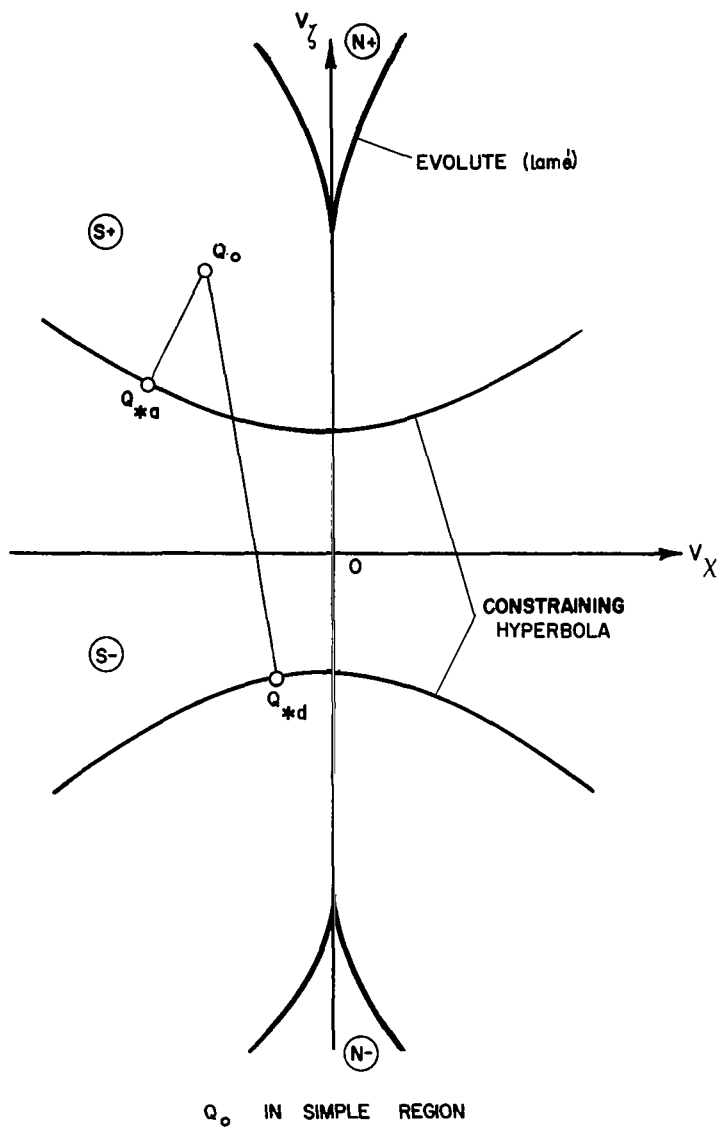
FIG. D-1 TYPICAL DISTRIBUTIONS OF THE ORTHOPOINTS
ON THE CONSTRAINING HYPERBOLA

Proof of the Existence of a Two-Impulse Extremum on the Optimal
Transfer Arc Pair

Assume f_1 and f_2 are continuous and twice differentiable.[†]
Consider a typical transfer arc pair of type (A). With
reference to Fig. E-1, the end points of the arc pair Q_{*1}
and Q_{*2} define a closed interval $[p, q]$. Since Q_{1*} and Q_{2*}
are the minimal points on this arc pair, we have:

At p:
$$\left. \begin{array}{l} f_1' = 0 \\ \\ f_2' < 0 \end{array} \right\} \quad f' = f_1' + f_2' < 0$$

At q:
$$\left. \begin{array}{l} f_1' > 0 \\ \\ f_2' = 0 \end{array} \right\} \quad f' = f_1' + f_2' > 0$$

Thus f' has opposite signs at the endpoints, hence there is
at least a local extremal f on the interval. Furthermore,
the absence of any stationary point and inflection point on f_1 and
f_2 in the interior of the interval shows that f_1' and f_2' are
monotonically increasing on the interval, and so is f'. Thus
the f' curve crosses the V_c - axis only once, and f'' is positive
throughout the interval. Consequently we conclude that,

There is one and only one interior extremal f

on the interval $[p, q]$, along the transfer arc pair

(A), and this extremum is a local minimum.

[†] This condition is actually met in any interval excluding the
origin, and where none of f_1 and f_2 vanishes.

Next, consider a typical transfer arc pair of type (B).
With reference to Fig. E-1B, we have, on the closed interval
$[p, q]$ defined by the endpoints Q_{1*a} and Q_{1*b} of the arc
pair:

At p:
$$\left. \begin{array}{l} f_1' = 0 \\ \\ f_2' < 0 \end{array} \right\} \quad f' = f_1' + f_2' < 0$$

At q:
$$\left. \begin{array}{l} f_1' = 0 \\ \\ f_2' < 0 \end{array} \right\} \quad f' = f_1' + f_2' < 0$$

Thus f' has the same sign at the endpoints, hence there is
either an even number of internal extrema of f or none.
Since, as assumed here, f_1 goes from one minimum to one
maximum on the interval, there exist one and only one point
of inflection on f_1, that is, there is one and only one
interior extremal f_1' on the interval. On the other hand,
in the absence of any stationary point and inflection point
other than the endpoint, f_2' is monotonically increasing, and
is negative throughout the interval. Consequently, f' first
increases and then decreases, with one and only one interior
extremum on the interval. Hence there are three possibilities:

1) f' cuts the V_c - axis at two points. There

   exists a pair of extremal values of f, one

   maximal and one minimal.

2) f' touches the axis. Then at the point of tangency, $f' = 0$ and $f'' = 0$, f is neither a maximum nor a minimum.

3) f' cuts the axis at no point. There exists no extremal f.

Consequently, we conclude that,

There is either one interior minimal f and one interior maximal f, or none on the interval [a, b], along the transfer arc pair (B).

The proof for the existence of a local maximum on the arc pair of type (D) is analogous to the proof for type (A).

OPTIMAL ARC PAIR
TYPE A
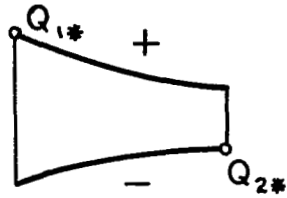
OPTIMAL ARC PAIR
TYPE B
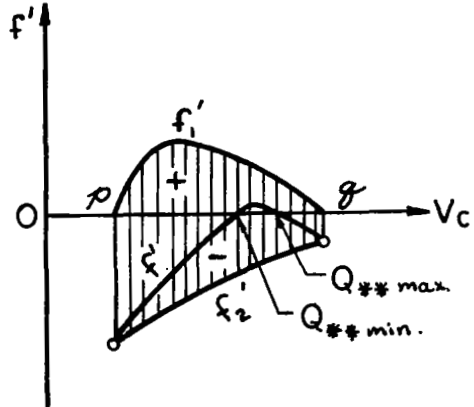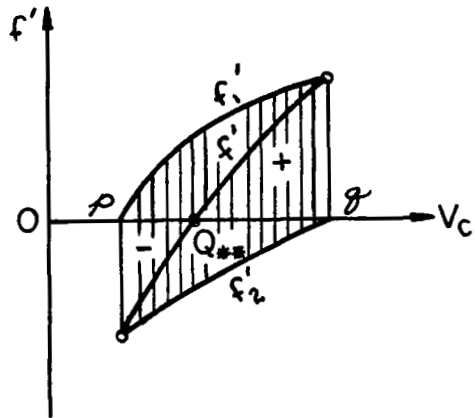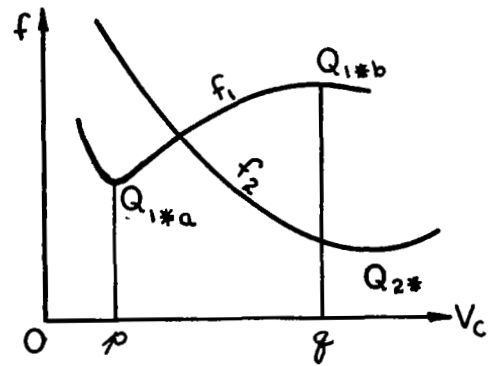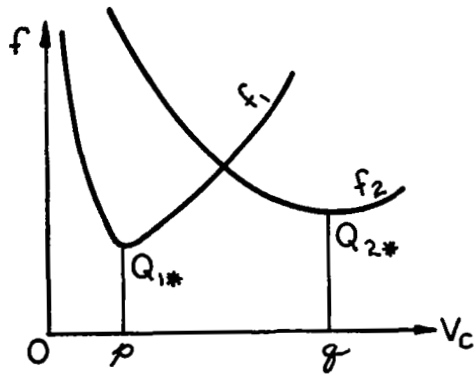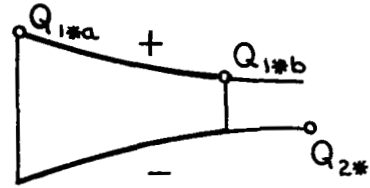
FIG. E-1   VARIATION OF THE IMPULSE FUNCTION AND ITS DERIVATIVE ALONG
AN OPTIMAL TRANSFER ARC PAIR

94

APPENDIX F

TABLE F: TERMINAL CONDITIONS AND THE MULTIPLICITY OF MINIMAL 2-IMPULSE SOLUTIONS

Case	Regional Locations of Terminal Velocity Points		Optimal Transfer Arc Pairs		Maximum Multiplicity		
	Q_{01}	Q_{02}	In One Kind and Sense	In Other Kind and Sense	In One Kind and Sense	In Other Kind and Sense	Both Kinds
1	S±	S±	(a,a)	(d,d)	1	1	2
2	S±	S∓	(a,d)	(d,a)	1	1	2
3	S±	N±	(a,a), (a,c)	(d,d)	2	1	3
4	S±	N∓	(a,d)	(d,a), (d,c)	1	2	3
5	N±	N±	(a,a), (a,c), (c,c)	(d,d)	3	1	4
6	N±	N∓	(a,d), (c,d)	(d,a), (d,c)	2	2	4

Note: For the double sign, all upper signs go together in each case, and so are all the lower signs.

NUMERICAL RESULTS

TABLE G-1A.   TRAJECTORY PARAMETERS FOR MINIMAL IMPULSE TRANSFERS: CIRCLE-TO-ELLIPSE

$$(\nu_{01} = 1.0, \ \nu_{02} = 0.5, \ \psi = 60°)$$

Distance Ratio $n = r_2/r_1$	Transfer Velocities						Angular Momenta		
	Chordal Components			Radial Components					
	V_{c*1}	V_{c*2}	V_{c**}	V_{R*1}	V_{R*2}	V_{R**}	h_{*1}	h_{*2}	h_{**}
0.2	1.7971	2.0854	1.8518	1.6999	1.4649	1.6497	.3396	.3941	.3499
0.3	1.4845	1.6931	1.5303	1.3304	1.1665	1.2906	.4339	.4949	.4473
0.4	1.3184	1.4615	1.3531	1.1020	.9941	1.0737	.5239	.5807	.5376
0.5	1.2251	1.3058	1.2460	.9425	.8842	.9266	.6125	.6529	.6230
0.6	1.1747	1.1933	1.1797	.8245	.8117	.8210	.7002	.7112	.7031
0.7	1.1514	1.1084	1.1401	.7351	.7636	.7424	.7853	.7560	.7776
0.8	1.1447	1.0427	1.1210	.6671	.7324	.6812	.8653	.7882	.8474
0.9	1.1476	.9912	1.1224	.6157	.7128	.6295	.9375	.8098	.9171
1.0	1.1547	.9505	1.1547	.5773	.7013	.5773	.9999	.8231	.9999
1.1	1.1632	.9183	1.1061	.5489	.6953	.5772	1.0517	.8303	1.0001
1.2	1.1713	.8927	1.0516	.5281	.6929	.5882	1.0931	.8332	.9814
1.3	1.1783	.8724	1.0009	.5130	.6929	.6040	1.1252	.8331	.9558
1.4	1.1839	.8563	.9581	.5023	.6945	.6207	1.1492	.8312	.9300
1.5	1.1880	.8434	.9233	.4948	.6970	.6367	1.1666	.8282	.9067
1.6	1.1911	.8330	.8955	.4897	.7002	.6514	1.1788	.8245	.8863
1.7	1.1931	.8247	.8732	.4863	.7036	.6645	1.1869	.8205	.8687
1.8	1.1943	.8180	.8554	.4843	.7072	.6762	1.1919	.8163	.8537
1.9	1.1950	.8126	.8411	.4833	.7108	.6867	1.1944	.8122	.8407
2.0	1.1952	.8082	.8294	.4830	.7143	.6960	1.1952	.8082	.8294

TABLE G-1B. TRAJECTORY PARAMETERS FOR MINIMAL IMPULSE TRANSFERS: CIRCLE TO HYPERBOLA

$$(\nu_{01} = 1.0, \ \nu_{02} = 1.5, \ \psi = 60°)$$

| Distance Ratio $n = r_2/r_1$ | Transfer Velocities | | | | | | Angular Momenta | | |
| | Chordal Components | | | Radial Components | | | | | |
	V_{c*1}	V_{c*2}	V_{c**}	V_{R*1}	V_{R*2}	V_{R**}	h_{*1}	h_{*2}	h_{**}
0.2	1.7971	3.4056	2.0122	1.6999	.8970	1.5182	.3396	.6436	.3802
0.3	1.4845	2.8388	1.7123	1.3304	.6957	1.1534	.4339	.8298	.5005
0.3999	1.3184	2.4924	1.5651	1.1020	.5829	.9283	.5239	.9903	.6219
0.4999	1.2251	2.2399	1.4966	.9425	.5155	.7715	.6125	1.1199	.7483
0.5999	1.1747	2.0350	1.4819	.8245	.4759	.6536	.7002	1.2129	.8833
0.6999	1.1514	1.8584	1.5148	.7351	.4554	.5587	.7853	1.2675	1.0332
0.7999	1.1447	1.7028	1.3519	.6671	.4485	.5649	.8653	1.2872	1.0219
0.8999	1.1475	1.5655	1.2192	.6157	.4513	.5795	.9375	1.2791	.9961
0.9999	1.1547	1.4460	1.1551	.5773	.4610	.5771	.9999	1.2522	1.0003
1.0999	1.1632	1.3436	1.1869	.5489	.4752	.5379	1.0517	1.2149	1.0732
1.1999	1.1713	1.2574	1.1899	.5281	.4919	.5199	1.0931	1.1735	1.1104
1.2999	1.1783	1.1856	1.1804	.5130	.5099	.5121	1.1252	1.1322	1.1272
1.3999	1.1839	1.1264	1.1651	.5023	.5279	.5104	1.1492	1.0935	1.1309
1.4999	1.1880	1.0778	1.1473	.4948	.5454	.5124	1.1666	1.0584	1.1267
1.5999	1.1911	1.0379	1.1290	.4897	.5620	.5166	1.1788	1.0272	1.1174
1.6999	1.1931	1.0050	1.1109	.4863	.5774	.5223	1.1869	.9998	1.1052
1.7999	1.1943	.9778	1.0937	.4843	.5916	.5289	1.1919	.9758	1.0915
1.8999	1.1950	.9552	1.0777	.4833	.6046	.5359	1.1944	.9548	1.0772
1.9999	1.1952	.9366	1.0631	.4830	.6164	.5430	1.1952	.9366	1.0631

TABLE G-2A. TERMINAL IMPULSES REQUIRED FOR MINIMAL IMPULSE TRANSFERS: CIRCLE-TO-ELLIPSE

$$(\nu_{01} = 1.0, \ \nu_{02} = 0.5, \ \psi = 60°)$$

Distance Ratio	T_{*1}			T_{*2}			T_{**}			Relative Saving	
	Initial	Final	Total $f_{*1} =$ $f_{1*1} +$	Initial	Final	Total $f_{*2} =$ $f_{1*2} +$	Initial	Final	Total $f_{**} =$ $f_{1**} +$	$\dfrac{f_{*1}-f_{**}}{f_{*1}}$	$\dfrac{f_{*2}-f_{**}}{f_{*2}}$
$n=r_2/r_1$	f_{1*1}	f_{2*1}	f_{2*1}	f_{1*2}	f_{2*2}	f_{2*2}	f_{1**}	f_{2**}	f_{2**}		
.2000	.6635	2.3606	3.0241	.8407	2.3105	3.1513	.6715	2.3426	3.0142	.0032	.0435
.3000	.5730	1.7479	2.3209	.6782	1.7140	2.3922	.5790	1.7342	2.3133	.0033	.0330
.3999	.4881	1.3565	1.8447	.5442	1.3368	1.8810	.4918	1.3479	1.8398	.0026	.0219
.4999	.4051	1.0760	1.4811	.4257	1.0684	1.4942	.4066	1.0720	1.4791	.0013	.0100
.5999	.3224	.8647	1.1871	.3237	.8642	1.1880	.3225	.8645	1.1870	.0001	.0008
.6999	.2398	.7081	.9479	.2484	.7051	.9535	.2403	.7067	.9471	.0008	.0066
.7999	.1577	.5989	.7567	.2175	.5785	.7960	.1613	.5908	.7522	.0059	.0551
.8999	.0774	.5320	.6094	.2369	.4768	.7137	.0847	.5169	.6017	.0126	.1569
.9999	.0000	.4999	.4999	.2870	.3944	.6814	.0000	.4999	.4999	.5444	.3343
1.0999	.0734	.4926	.5661	.3473	.3271	.6745	.1048	.4356	.5405	.0452	.1986
1.1999	.1421	.4999	.6421	.4078	.2719	.6798	.2113	.3686	.5800	.0967	.1468
1.2999	.2057	.5142	.7199	.4649	.2261	.6910	.3099	.3061	.6161	.1442	.1084
1.3999	.2641	.5307	.7949	.5171	.1879	.7050	.3968	.2516	.6484	.1842	.0803
1.4999	.3175	.5469	.8645	.5644	.1557	.7202	.4715	.2055	.6771	.2167	.0598
1.5999	.3662	.5618	.9280	.6071	.1284	.7355	.5356	.1670	.7027	.2428	.0446
1.6999	.4105	.5749	.9854	.6455	.1051	.7506	.5908	.1347	.7255	.2636	.0333
1.7999	.4508	.5861	1.0369	.6801	.0850	.7651	.6385	.1076	.7461	.2803	.0248
1.8999	.4875	.5956	1.0831	.7113	.0676	.7790	.6801	.0847	.7648	.2938	.0182
1.9999	.5202	.6034	1.1237	.7390	.0531	.7921	.7166	.0650	.7815	.3045	.0133

TABLE G2B.   TERMINAL IMPULSES REQUIRED FOR MINIMAL IMPULSE TRANSFERS: CIRCLE-TO-HYPERBOLA

$$(\nu_{01} = 1.0, \ \nu_{02} = 1.5, \ \psi = 60°)$$

Distance Ratio	T_{*1}			T_{*2}			T_{**}			Relative Saving	
	Initial	Final	Total $f_{*1} =$ $f_{1*1} +$	Initial	Final	Total $f_{*2} =$ $f_{1*2} +$	Initial	Final	Total $f_{**} =$ $f_{1**} +$	$\dfrac{f_{*1}-f_{**}}{f_{*1}}$	$\dfrac{f_{*2}-f_{**}}{f_{*2}}$
$n=r_2/r_1$	f_{1*1}	f_{2*1}	f_{2*1}	f_{1*2}	f_{2*2}	f_{2*2}	f_{1**}	f_{2**}	f_{2**}		
.2000	.6635	2.8245	3.4881	2.4730	2.0164	4.4894	0.7704	2.6170	3.3875	.0288	.2454
.3000	.5730	2.1071	2.6801	2.0263	1.3348	3.3611	0.6956	1.8742	2.5699	.0411	.2354
.3999	.4881	1.6426	2.1308	1.7042	.8750	2.5793	0.6331	1.3764	2.0096	.0568	.2208
.4999	.4051	1.3010	1.7061	1.4294	.5300	1.9594	0.5818	0.9932	1.5751	.0768	.1961
.5999	.3224	1.0333	1.3558	1.1774	.2570	1.4345	0.5489	0.6704	1.2193	.1007	.1500
.6999	.2398	.8226	1.0624	.9424	.0413	.9838	0.5500	0.3845	.9345	.1203	.0500
.7999	.1577	.6633	.8210	.7254	.1283	.8538	0.3208	0.4179	.7387	.1002	.1347
.8999	.0774	.5559	.6333	.5306	.2600	.7906	0.1234	0.4791	.6026	.0485	.2378
.9999	.0000	.5000	.5000	.3637	.3605	.7242	0.0003	0.4996	.4999	.0000	.3097
1.0999	.0734	.4874	.5608	.2365	.4361	.6726	0.0795	0.4750	.5545	.0113	.1755
1.1999	.1421	.5033	.6455	.1781	.4921	.6703	0.1440	0.4990	.6431	.0037	.0405
1.2999	.2057	.5334	.7392	.2059	.5333	.7393	0.2057	0.5334	.7392	.0000	.0001
1.3999	.2641	.5680	.8322	.2738	.5633	.8371	0.2652	0.5654	.8307	.0018	.0077
1.4999	.3175	.6019	.9195	.3467	.5848	.9315	0.3215	0.5918	.9134	.0066	.0194
1.5999	.3662	.6329	.9992	.4146	.5999	1.0146	0.3742	0.6122	.9865	.0127	.0277
1.6999	.4105	.6602	1.0707	.4755	.6104	1.0859	0.4230	0.6273	1.0504	.0190	.0327
1.7999	.4508	.6837	1.1345	.5295	.6172	1.1468	0.4679	0.6381	1.1060	.0251	.0355
1.8999	.4875	.7037	1.1912	.5774	.6214	1.1988	0.5091	0.6454	1.1545	.0308	.0369
1.9999	.5202	.7197	1.2399	.6190	.6228	1.2419	0.5459	0.6493	1.1952	.0360	.0375